Title

Excitation Spillover from PSII to PSI Measured in Leaves at 77K

Running Title

Spillover from PSII to PSI in Leaves

Corresponding Author
Ichiro Terashima
Institute of Agro-ecosystem Services,
Graduate School of Agricultural and Life Science,
The University of Tokyo,
Midori machi 1-1-1, Nishi-Tokyo City, Tokyo, 188-0002 JAPAN
TEL: +81-42-463-1611
FAX: +81-42-463-4391
E-mail: terashimaichiro6@gmail.com

Subject Areas
(5) Photosynthesis, Respiration and Bioenergetics
(2) Environmental and Stress Responses

Number of black and white figures:4
Number of color figures:4 (including a figure for the appendix)
Supplementary materials: 6 figures.

Title

Excitation Spillover from PSII to PSI in Leaves at 77K

Running Title

Spillover from PSII to PSI in Leaves

Names and addresses of authors

Ichiro Terashima[1,4*], Riichi Oguchi[1,5], Kimie Atsuzawa[2], Yasuko Kaneko[3] and Masaru Kono[1,6*]

[1]Department of Biological Sciences, School of Science, The University of Tokyo, Tokyo, 113-0033, Japan
[2]Comprehensive Analysis Center for Science, Saitama University, Saitama, 338-8570, Japan
[3]Department of Natural Science, Faculty of Education, Saitama University, 338-8570, Japan

Present addresses
[4]Institute of Sustainable Agro-ecosystem Services, Graduate School of Agricultural and Life Sciences, The University of Tokyo. Nishi-Tokyo 188-0002, Japan
[5]Botanical Gardens, Osaka Metropolitan University, Katano 576-0004, Japan
[6]Astrobiology Center, National Institutes of Natural Sciences, Mitaka 181-8588, Japan

*Corresponding authors
Ichiro Terashima (terashimaichiro6@gmail.com)
Masaru Kono (konom07@bs.s.u-tokyo.ac.jp)

ABSTRACT

Heterogeneous distribution of PSI and PSII in thick grana in shade chloroplasts is believed to hinder spillover of chlorophyll excitations from PSII to PSI. To examine this dogma, we measured fluorescence induction at 77K at 690 nm (PSII) and 760 nm (PSI) in the leaf discs of spinach, cucumber, and shade tolerant *Alocasia odora*, grown at high and low light, and quantified their spillover capacities. PSI fluorescence (F_{I}) consists of the intrinsic PSI fluorescence ($F_{\mathrm{I}\alpha}$) and fluorescence caused by excitations spilt over from PSII ($F_{\mathrm{I}\beta}$). When F_{I} *and* F_{II} parameters between State 1 and State 2, induced by weak PSI and PSII light, were compared, PSII maximum fluorescence ($F_{\mathrm{II}m}$) was greater and $F_{\mathrm{I}\alpha}$ was smaller in State 1 by up to 30 %. The spillover ratio, $F_{\mathrm{I}\beta}/F_{\mathrm{I}m}$, ranging from 0.25 to 0.4, was greater in State 1. In a barley *b*-less mutant, both $F_{\mathrm{II}m}$ and $F_{\mathrm{I}\alpha}$ were insensitive to PSI or PSII light, and $F_{\mathrm{I}\beta}/F_{\mathrm{I}m}$ was 0.33. *A. odora* leaf discs that were frozen after NPQ induction showed lower $F_{\mathrm{I}\beta}$ and $F_{\mathrm{I}\beta}/F_{\mathrm{I}m}$ than the dark controls, while $F_{\mathrm{I}\alpha}$ did not change. In contrast to the dogma, the spillover ratios were not lower in low light grown leaves. Although extensive grana in low light grown plants would hint that PSII and PSI are too separated for spillover, in chloroplasts in high and low light grown *A. odora* leaves, the ratio of non-appressed thylakoid membranes/total thylakoid membranes was little affected by growth light and more than 40%. (245 words)

Keywords: fluorescence induction, grana, state transitions, sun/shade chloroplasts

Introduction

Land plants are exposed to various light fluctuations. Sudden changes in the photon flux density (PFD) from low to high levels often cause photoinhibition in PSII and PSI (for a recent review, see Kono et al. 2024).

Plants have evolved several mechanisms to protect photosystems from photoinhibition. Leaf and chloroplast movements are important mechanisms (Kasahara et al. 2002, Pastenes et al. 2005), although these are beyond the present scope. The non-photochemical quenching (NPQ), by which excitations (excited chlorophylls, hereafter abbreviated as Chl*s) are dissipated as heat, has been studied most intensively. Changes in the protein structure and the energy levels of the pigments in the PSII antenna systems due to protonation of PsbS protein and conversion of violaxanthin via antheraxanthin to zeaxanthin, are responsible for NPQ induction (Bassi and Dall'Osto 2021). It has been proposed that, during NPQ induction, some light harvesting chlorophyll protein complexes are clustered and functionally separated from the PSII core complexes (Ruban et al. 2012). Then, Chl*s in such antenna clusters are dissipated as heat. It takes 5 to 10 min for considerable induction of NPQ at ordinary temperatures. Full conversion of violaxanthin to zeaxanthin takes some more time (Bassi and Dall'Osto 2021). Conversely, when the PFD level is lowered, NPQ is relaxed and thereby loss of Chl*s as heat is suppressed. The relaxation processes take several minutes as well.

For efficient photosynthesis in fluctuating light, NPQ should be induced and relaxed as rapidly as possible. Kromdijk et al. (2016) overexpressed three components involved in the induction and relaxation processes of NPQ, violaxanthin de-epoxidase, PsbS, and zeaxanthin epoxidase, in *Nicotiana tabacum* (tobacco). When gas exchanges of such leaves were assessed in the laboratory using red and blue LEDs as the actinic light, the NPQ relaxation processes were accelerated. A field experiment showed that these plants grew better than the wild type in the field where light fluctuated. Three lines of *Arabidopsis thaliana* overexpressing these three components showed faster NPQ induction and relaxation in the laboratory. However, these lines did not grow better than the wild type in a natural light greenhouse. In an artificial fluctuating light in a growth chamber, growth of these lines was even inferior to that of the wild type (Garcia-Molina and Leister 2020). Although the discrepancy between tobacco and *A. thaliana* lines has not been elucidated, the strong induction of NPQ might exert a negative effect on photosynthetic production *in A. thaliana* under the experimental conditions adopted by Garcia-Molina and Leister (2020).

We recently found that far-red (FR) light accelerates NPQ relaxation in *A. thaliana* (Kono et al. 2020). We also found that the H^+/K^+ antiporter in thylakoid membranes (KEA3) is involved in the NPQ relaxation and that the KEA3 is activated by FR light (Kono et al. unpublished observation). The results of Kromdijk et al. (2016) in the field, therefore, should have reflected this FR light effect on the rapid NPQ relaxation, because FR light is abundant in the field.

The state transitions realise balanced Chl* distribution between PSII and PSI by adjusting allocation of mobile LHCIIs between these photosystems. Thus, the mechanisms are important for the linear electron transport to be smoothly driven. The LHCII movements from PSII to PSI and from PSII to PSI are caused by the phosphorylation and dephosphorylation of LHCIIs and the PSII core, and the responsible kinases have been identified. The state transitions were once proposed to play roles in protecting PSII from photoinhibition in high light (Horton and Lee

1985, Anderson and Andersson 1988, Bellafiore et al. 2005). However, these kinases are inactivated in high light *in vivo* (Rintamäki et al. 1997, Pursiheimo et al. 1998). Thus, these kinases would not be involved in avoidance of high light stresses. In the continuous growth light, the mutant deficient in one of these kinases, *stn7*, grew well. Thus, LHCII phosphorylation may not be needed in high light. However, *stn7* did not grow well in the fluctuating light. Thus, LHCII phosphorylation may play a role in acclimation to the fluctuating light (Grieco et al. 2012).

The spillover denotes transfer of Chl*s from PSII to PSI. Analyses of fluorescence induction at 77K revealed that induction of PSI fluorescence occurred synchronously with that of PSII. When PSII reaction centres close, Chl*s are transferred from PSII to PSI. Some spillover also occurs in the absence of closed PSII. Therefore, the instantaneous PSI fluorescence (F_{I0}) contains a fraction exited by Chl*s spilt over from PSII. This phenomenon was noticed in 1960's (Murata 1969). Theoretical analyses were also made (Kitajima and Butler 1975a, b, Strasser and Butler 1977a, b). Since the spillover prevents singlet excitations (^{S}Chl*s) from haunting around the closed PSII reaction centres, the conversion of ^{S}Chl*s to triplet ones (^{T}Chl*s) is also suppressed. Since ^{T}Chl*s tend to transfer energy to $^{T}O_2$ to produce $^{S}O_2$, the spillover suppresses $^{S}O_2$ production. Although the energy level of ^{T}Chl* is lower than that of ^{S}Chl*, the lifetime of ^{T}Chl* is longer than that of ^{S}Chl* by 3 orders of magnitude (Khorobrykh et al. 2020). Thus, once ^{T}Chl* is formed, the chance of energy transfer from ^{T}Chl* to $^{T}O_2$ increases. Hence, the spillover alleviates PSII photoinhibition by suppressing $^{S}O_2$ formation. When vigorous spillover occurs, PSII reaction centres tend to be closed and the electron flow from PSII to PSI is suppressed. Then, Chl*s transferred from PSII to PSI oxidise P700 to P700^{+}, which is the key component for protection of PSI from photoinhibition (Miyake 2020). Therefore, the spillover would protect not only PSII but also PSI from photoinhibition (Terashima et al. 2021, Kono et al. 2024).

The extent of NPQ is smaller in shade plant leaves than in sun plant leaves, mostly due to the smaller pool size per leaf area of xanthophyll cycle carotenoids in shade plant leaves (Demmig-Adams and Adams 2006). Shade plants in the canopy understories are often exposed to sunflecks (Pearcy 1990) or sunpatches (Smith and Berry 2013). To avoid photoinhibition due to such drastic changes in PFD, spillover would be more efficient than NPQ, because spillover occurs instantaneously while induction of NPQ requires several minutes. Shade plant leaves, therefore, must rely more on the spillover than sun plant leaves for avoiding photoinhibition.

The spillover is believed to occur in the megacomplexes which include the PSI, PSII and LHC complexes (Yokono et al. 2015, Ifuku 2023, Kim et al. 2023). These megacomplexes have two-dimensional structures in the thylakoid membrane. Then, Chl*s are transferred within the megacomplexes in the single membrane. The chloroplast thylakoid membranes are categorized into the appressed or non-appressed membranes. The appressed membranes are located inside the grana in contact with other appressed membranes, while the non-appressed membranes face the stroma and form the inter-grana thylakoids or the grana surface membranes. In the thylakoid membranes, there are four major protein complexes, and their distributions are heterogeneous (Anderson and Andersson 1988). PSII complexes are mainly located in the appressed membranes, while PSI complexes and H^{+}-ATPases are mainly located in the non-appressed membranes. Given that PSII in the appressed membranes are located distant from PSI in the non-appressed

membranes and that the spillover occurs within the megacomplexes, it would be unlikely for Chl*s to be transferred from PSII in one membrane to PSI in a separate membrane. However, the transfer of Chl*s across the membranes was once claimed to occur based on measurements of electrogenicity in thylakoid preparations (Trrisl et al. 1987).

It is known that the chloroplast morphologies are different between sun and shade plants. Grana are generally thicker and contain more thylakoids in shade plant chloroplasts (Anderson 1986, Björkman 1981). The similar trends have been reported for high- and low-light grown plants of the same species (Anderson 1986, Björkman 1981). These morphological features imply that spillover would occur more easily in sun-type chloroplasts that have thinner grana. Chow et al. (1988) showed an electron micrograph of gigantic grana in a leaf of low-light grown *Alocasia macrorrhiza*, a shade-tolerant Araceae species. The number of thylakoids per granum in the gigantic grana exceeded 100. These impressive grana suggest that the spillover of Chl*s from PSII to PSI might be hampered in such chloroplasts.

In a recent paper, in which the spillover in Scots pine leaves was detected by the time-resolved fluorescence analysis, the authors claimed that the increase in the spillover was accompanied by the decrease in the number of thylakoids per granum or by thylakoid de-stacking (Bag et al. 2020). Yokono et al. (2019) surveyed existence of the megacomplexes in various green plants and found that sun plants accumulate more PSI-PSII megacomplexes than shade plants. They also found a tendency that PSI of sun plants had deeper traps (low-energy chlorophylls) to receive excitation energy and showed PSI fluorescence maxima at wavelengths longer than 730 nm. Unfortunately, typical shade-tolerant plants were not included in their plant materials (Table 1 of Yokono et al. 2019). Based on spectroscopic evidence of existence of deep-trap chlorophyll *a* in leaves of a shade-tolerant *Alocasia odora*, we proposed that the shade-tolerant plants should also have PSI-PSII megacomplexes and, due to the deep-trap Chl*a*, spillover of the excitation energy from PSII to PSI should contribute to formation of $P700^+$ in high light (Terashima et al. 2021, Kono et al. 2024).

In the present study, we grew sun species such as spinach (*Spinacia oleracea*) and cucumber (*Cucumis sativus*), and a shade-tolerant species, *A. odora* at different light levels. We also grew a wild type and a chlorophyll *b*-less mutant of barley (*Hordeum vulgare*). Using leaf discs of these plants frozen at 77 K, we measured the induction of PSII fluorescence at 690 nm and that of PSI fluorescence at 760 nm. We analyzed PSI fluorescence into the fraction corresponding to the PSI fluorescence caused by Chl*s spilt over from PSII and the intrinsic PSI fluorescence. The ratios were compared among the species and among the growth light levels. Considerable spillover was detected in the leaves of low light grown *A. odora*. Moreover, the spillover was not necessarily greater in high light grown plants. The barley *b*-less mutant also showed considerable spillover.

Since the differences in ultrastructure of between the chloroplasts from high and low light grown *A. macrorrhiza* (Chow et al. 1988) were intriguing, we quantitatively analyzed the thylakoid ultrastructure of *A. odora* to elucidate the interrelationship between the ratio of non-appressed thylakoid membranes to total thylakoid membranes, thylakoid stacking, and the spillover.

Results

Fluorescence induction

The leaf disc placed on wet paper was illuminated with weak light from LEDs peaked at 720 nm (PSI light) or those at 470 nm (PSII light) at a photon flux density of 10 or 5 μmol m^{-2} s^{-2} for at least 30 min to allow transitions to State 1 or State 2, respectively, and frozen to 77 K. Induction of fluorescence excited by blue light at 460 nm at 50 μmol m^{-2} s^{-2} was measured either at 690 nm or 760 nm for PSII fluorescence (F_{II}) or PSI fluorescence (F_I) at 1 ms time intervals for 30 s. For the measurement system, see Materials and Methods, and Fig. S1. F_{II} and F_I both showed typical induction curves (Fig. 1A). It took about 5 s to attain F_m levels. F_v/F_m levels of PSII fluorescence (F_{IIv}/F_{IIm}) ranged from 0.76 to 0.85, except for somewhat lower values in *b*-less barley mutant (Table 1). When F_I level was plotted against F_{II} level, a linear line was obtained (Fig. 1B). The linear relationship is prerequisite for our assumption that the induction in F_I is due to the spillover from PSII.

We fitted the induction time course, $F_{II}(t)$, to the equation (Eq. 8 in Materials and Methods) and obtained $t_{1/2}$ at the time point where the fluorescence level was $F_{II}(t_{1/2}) = F_{II0} + (F_{IIm} - F_{II0})/2$. The data of chlorophyll (Chl) contents and Chl a/b ratios, F_{IIv}/ F_{IIm} and $F_{II}(t_{1/2})$ in the leaf discs are shown in Table 1. Because PSII fluorescence is reabsorbed by chlorophylls, the absolute levels of PSII fluorescence should not be compared. However, for the set of materials from the same leave, the effects of state transitions can be examined (Table 1). Mobile LHCIIs would move from PSII to PSI in State 2 light and *vice versa* in State 1 light. Then, faster F_{II} induction was expected to occur in State 1, because antenna size per PSII reaction centre would increase in State 1. This tendency was observed in all the samples. When HL and LL leaves were compared, Chl *a*/*b* was lower in LL leaves, indicating that LHCIIs were more abundant in LL leaves. Thus, the induction was expected to be faster in LL leaves. As expected, this was the case in all materials.

Effects of growth light and State transitions on F_{IIm}, $F_{I\alpha}$, F_{Im} and F_{Iv}/ F_{Im} are summarized in Table 2. Because the present State 2 light was blue, chloroplasts might accumulate to cell walls parallel to the leaf surface during the pre-treatment for 30 min (Cazzaniga et al. 2013). Then, F_{IIm} might be enhanced. However, when compared for the same leaf materials, F_{IIm} was always greater in State 1 (Table 2), as consistent with the view of LHCII movement from PSI to PSII in State 1 light. As already shown in Fig. 1, F_I showed induction. We assume that the induction is attributed to the spillover of Chl*s from PSII. We also assumed that the spillover occurs even when there were no closed PSII reaction centres. Then, $F_I(t)$ is expressed as $F_I(t) = F_{I\alpha} + \beta F_{II}(t)$, where $F_{I\alpha}$ is the intrinsic PSI fluorescence, and β is the spillover coefficient, calculated as F_{Iv}/F_{IIv} (Kitajima and Butler 1985, Butler and Kitajima 1985, Strasser and Butler 1987a, b). This is Eq. 6 (for detail, see Materials and Methods). For an explanation of the interrelationships between F_I and F_{II}, see Fig. S2. At 760 nm, F_I would be hardly reabsorbed. However, PSI fluorescence also saturates with the increases in the chlorophyll content in leaf discs because the light absorptance increases (See Fig. S3). Thus, the values were compared only for the same materials.

$F_{I\alpha}$, was consistently greater in State 2 light, although the differences were not always statistically significant. Chloroplast accumulation to the horizontal cell

walls might contribute to the increase in $F_{I\alpha}$ by the State 2 light pretreatment. The spillover was however greater in State 1. The balance of these determined F_{Im}. In cucumber HL and barley WT, F_{Im} were greater in State 2, while in other materials, the differences between State 1 and 2 were not statistically significant. On the other hand, F_{Iv}/F_{Im} were significantly greater in State 1 in all materials, reflecting the greater spillover from PSII.

The proportions of the spillover in PSI fluorescence, $F_{I\beta}/F_{Im}$, which is equal to $F_{I\beta}/(F_{I\alpha} + F_{I\beta})$, are shown in Fig. 2 (see also Fig. S2). As was expected from F_{Iv}/F_{Im} data in Table 2, $F_{I\beta}/(F_{I\alpha} + F_{I\beta})$ was consistently greater in State 1 light. When HL- and LL-discs were compared, the levels were comparable in spinach. But in cucumber and *A. odora*, the values were significantly greater in LL-discs. The highest $F_{I\beta}/(F_{I\alpha} + F_{I\beta})$ values around 0.4 were observed in HL- and LL-spinach, and LL-cucumber in State 1. The leaves of shade tolerant *A. odora* showed the value of more than 0.3 in State 1. The *b*-less barley mutant also showed considerable spillover above 0.3. It is noteworthy that there were no effects of the State light on fluorescence data in the *b*-less barley, in which LHCIIs are mostly absent.

Effects of NPQ

Effects of NPQ formation on spillover was examined in the leaf discs from LL-*A. odora* leaf discs (Table 3 and Fig. 3). After the induction of NPQ by a white light at 700 µmol m^{-2} s^{-1} for 270 s at a room temperature of ca. 23℃, NPQ values, (F_{IIm}-F_{IIm}')/ F_{IIm}', were measured. Then, weak PSI light (at 720 nm) was given for 10 s to oxidise the acceptor side of PSII, and the leaf disc was frozen.

Compared with typical sun plants, NPQ is usually modest in shade tolerant plants due to the low pool size of xanthophyll cycle carotenoids (Demmig-Adams and Adams III 2006). Although LL-grown *A. odora* was used and the actinic light was moderate, NPQ levels after the NPQ induction were substantial (Table 3). The values between the samples for PSI fluorescence measurements and those for PSII fluorescence measurements were not statistically different (Table 3). The data in Fig. 3, showing smaller $F_{I\beta}$ and $F_{I\beta}/(F_{I\alpha} + F_{I\beta})$ in the NPQ-induced leaf discs, indicate that the spillover of Chl*s from PSII to PSI was decreased by the NPQ induction. $F_{I\beta}/(F_{I\alpha} + F_{I\beta})$ in the dark treated control was 0.3, which was similar to the value in State 2 light in LL-*A. odora* (Fig. 2), which was shown by Weis (1985). It is also noteworthy that $F_{I\alpha}$ was unaffected by NPQ.

Effects of $P700^+$ on PSI intrinsic fluorescence

The pulse-modulated measuring/actinic beam for preferential excitation of PSI was peaked at 700 nm and at the PFD level of 0.07 µmol m^{-2} s^{-1}. Changes in the intrinsic PSI fluorescence are shown in Fig. 4. After 15 s from the onset of recording at 4 ms intervals, the measuring/actinic light was on. First, no damping (noise reduction circuit) was used to examine whether there was an induction phenomenon in the PSI intrinsic fluorescence. Even though the measuring/actinic light was very weak, no induction processes were observed in both *A. odora* and spinach (Fig. 4A and B) When an unmodulated blue light at 58 µmol m^{-2} s^{-1} was added, the fluorescence level increased to a small extent. This increase was not synchronized with the increase in $P700^+$ (Fig. 4C and D). Moreover, the fluorescence levels did not respond to further increases in the PFD level.

Therefore, the increase in the 'PSI' fluorescence on the addition of the blue light would not be related to $P700^+$. Instead, a slight increase in the 'PSI' fluorescence upon the blue light illumination might reflect the PSII fluorescence induction and fluorescence caused by spillover Chl*s from PSII to PSI. It is probable that the light used for PSI excitation slightly excited PSII. PSII reduction proceeded very slowly, because the measuring/actinic beam had a narrow peak at 700 nm and was very weak. Judging from the induction shown in Fig.1, PSII would be fully reduced within 5 s upon illumination of the blue light at 58 μmol m^{-2} s^{-1}. Thus, the PSII fluorescence level excited by the modulated measuring/actinic light would increase. PSI fluorescence caused by the spillover from PSII contributed to this small increase. Once PSII reaction centres were all reduced, further increases in the 'PSI' fluorescence attributable to closure of PSII were not observed even in the stronger actinic lights.

$P700^+$ increased slowly in the weak measuring/actinic light and more rapidly with 58 and 360 μmol m^{-2} s^{-1} blue light (Fig. 4 and D). A further increase in the actinic light to 3000 μmol m^{-2} s^{-1} did not cause a notable increase in $P700^+$, indicating that the $P700^+$ level was nearly saturated. When the 'PSI' traces are compared with the $P700^+$, there were no indications of fluorescence quenching or fluorescence increases with the increase in $P700^+$. Upon illumination with 3000 μmol m^{-2} s^{-1}light, some decreases in 'PSI' fluorescence were observed both in spinach and *A. odora*.

For the Förster resonance transition of the excitation from the excited pigment A to B to occur, the fluorescence emission spectrum of A should overlap with the absorption spectrum of B. The probability is also proportional to the inverse of the sixth power of the distance between these pigments (Blankenship 2021). Because $P700^+$ has a broad absorption band (Inoue et al. 1973), which well overlaps with the PSI fluorescence emission spectrum from red chlorophylls, Förster resonance transition would be possible from Chl*s to $P700^+$. When this transition occurs efficiently, quenching of PSI fluorescence with the increase in P700+ may be expected. However, this was not the case in the present materials.

Effects of PSII fluorescence on PSI fluorescence

Because the F_{II} emission spectrum overlaps with the absorption band of Chl *a*, some F_{II} is absorbed by long waveband Chl *a* molecules in PSI. Then, F_I would be caused not only by the spillover Chl*s from PSII to PSI but also by F_{II} *per se* rather directly.

In the present measuring system, the measuring/actinic light was illuminated from one side of the leaf disc and fluorescence emitted from the same side was measured (Fig. S1). Chlorophylls were excited with the pulse-modulated blue light at 460 nm and F_{II} and F_I were measured at 690 and 760 nm. The ratio of the F_I excited by F_{II} to the F_I directly driven by the blue light was estimated using a simple model (see the Appendix and Fig. 8). The calculations indicate that this ratio should increase with the Chl concentration per leaf area or the Chl concentration in the thylakoid suspension (Fig. S4). If excitation of PSI by F_{II} is substantial, then F_{Iv}/F_{Im} should increase with the chlorophyll concentration. We examined this possibility, using the suspensions of spinach thylakoids of varying Chlorophyll concentrations in a 3-mm thick aluminum cup (see Fig. 5A and Fig. S1). We also plotted the F_{Iv}/F_{Im} against the chlorophyll content in the leaf discs. We found no dependences of F_{Iv}/F_{Im} on the chlorophyll content in the sample (Fig.

5A and B). These results indicate that the effect of PSI excitation by F_{II} was negligibly small for the present examination. This would be attributed to low PSII fluorescence yield *in vivo*, which is only a few percent (Latimer et al. 1957, Lamb et al. 2018).

Chloroplast ultrastructure of *A. odora*

In Fig. 6, electron micrographs of the chloroplasts in the leaves from the *A. odora* plants grown at 180 (HL) and 10 (LL) μmol m^{-2} s^{-1} are shown. These chloroplasts were from the first cell layers in the palisade tissues to avoid the effects of intra-leaf light gradient (Skene 1974, Terashima et al. 1986, Terashima and Hikosaka 1995). Thylakoid membranes per unit volume were more abundant in LL chloroplasts than in HL chloroplasts. Near the chloroplasts, peroxisomes (P) and mitochondria (M) were observed in both samples (Fig. 6 A and B). Starch grains (S) and lipid components (plastoglobules) were more conspicuous in HL chloroplasts (Fig. 6 A) than in LL chloroplasts (Fig. 6B). In both samples, directions of the grana stacks were variable. Thus, both circular face views and side views of grana stacks were seen within the same sections. The diameters of grana were greater in the LL chloroplasts than in HL chloroplasts. The number of thylakoids per granum was somewhat smaller in LL chloroplasts than in HL chloroplasts. In HL chloroplasts, huge grana with numerous thylakoids were occasionally observed. In these huge grana, some thylakoids were swollen, and, in places, stackings were not tight. In both chloroplasts, there were abundant inter-grana thylakoids.

In Fig. 7A. the total length of thylakoid membranes per 1 μm^2 of the ultrathin sections are shown. As already described above (Fig. 6), thylakoid membranes were more packed in the LL chloroplasts than in HL chloroplasts. The quantitative analysis of the ratios of non-appressed membrane/total thylakoid membranes (Fig. 7B) revealed that the ratios were similar between HL and LL chloroplasts because the inter-grana thylakoids were abundant in both HL and LL leaves.

Discussion

Quantitative analyses of the spillover

Recent studies on the spillover have been employing the time-resolved fluorescence spectral analysis (Yokono 2015, Bag et al. 2020). Although time scale of spillover and the roles of respective pigments have been clarified by this method, quantitative analyses of the quantum yield of spillover may not be feasible. For example, it is hard to estimate how much of Chl*s move from PSII to PSI, although an attempt to measure the quantum yield of spillover in mixtures of cyanobacterial PSI and PSII preparations based on the steady-state and time-resolved fluorescence spectroscopy has been recently proposed (Akhtar et al. 2024). Classically, slower changes of fluorescence at 77K were analyzed (Kitajima and Butler 1975a, b, Strasser and Butler 1977a, b). The present study followed these classics.

As shown in Fig. 1, in the time scale of the present study, inductions of PSI and PSII fluorescence were synchronous as has been shown (Kitajima and Bulter 1975b). Thus, we attributed the main part of PSI induction to the spillover of excitations from PSII. We also assumed that spillover occurs irrespective of the absence or presence of closed PSII (Kitajima and Bulter 1975 a, b, Strasser and Butler 1977b). The excitation spectrum and emission spectrum of F_{II0} (Franck et al. 2002), it is clear that the spillover occurs at F_0. For the diagram of these relationships between F_I and F_{II}, see Fig. S2.

As shown in Fig. 1 and Tables 1 and 2, F_{IIm} was greater in PSI light (State 1), while $F_{I\alpha}$ was greater in PSII light (State 2). Induction time ($t_{1/2}$) was shorter in the leaves grown at lower irradiances. Given that the antenna complexes per reaction centre is more abundant in the low-light acclimated chloroplasts, which is inferred by lower Chl *a*/*b* ratios in LL materials than in HL materials, the faster induction in the low-light grown materials is reasonable. When fluorescence levels were compared between State 1 and State 2, the induction tended to be faster in State 1.

F_{IIm} was greater after the State 1 treatment in all materials (Table 2). However, F_{Im} was not necessarily greater after the State 2 treatment, because the contribution of the spillover was considerable. When the component of PSII spillover was subtracted, the intrinsic PSI fluorescence ($F_{I\alpha}$) was always greater in State 1.

The absolute contribution of spillover to F_I is summarized in Fig. 2. The lowest value was recorded for the HL grown *A. odora* treated in State 2 light. However, this was still more than 0.25. The highest values approached nearly 0.40 in State 1 light. The main purpose of the present study was to examine whether the spillover occurs in LL- acclimated chloroplasts. This has been confirmed. Considerable spillover occurred in the shade tolerant plant *A. odora*, and the spillover ratio in this plant was greater in the LL-leaf than in the HL-leaf. In cucumber as well, the LL-leaf showed higher spillover ratios.

When NPQ was developed, the spillover from PSII to PSI became smaller. It is also noteworthy that $F_{I\alpha}$ was unaffected, indicating that NPQ did not develop in the PSI antennae. Or its effect was negligibly small. In *Chlamydomonas*, the protonated LHCSR3 is involved in energy dissipation in both PSI and PSII antennae (Tokutsu et al.2013, Girolomoni et al. 2019). However, its close homologs are not found in land plants. Although the nil effect of NPQ on $F_{I\alpha}$ (Fig.

3) might not be regarded conclusive, as far as the leaf discs of the present plant materials treated with low light for State changes or treated in the dark, $F_{I\alpha}$ can be dealt with as a constant.

It has been shown that the excited state of deep-trapped chlorophyll *a* is quenched by $P700^+$ time-resolved fluorescence spectral analysis (Yokono et al. 2019). It is inferred that PSI fluorescence is quenched in the presence of $P700^+$. On the other hand, in the P700-enriched particles (Ikegami 1976) and the PSI preparation (Wientjes and Croce 2012), $P700^+$ increases the PSI fluorescence level. Although Ikegami (1976) found a considerable increase in PSI fluorescence in his PSI particle, having the Chl/P700 ratio of 7, he argued that this much increase would be hidden in the thylakoids. Wientjes and Groce (2012) detected a 4% increase in PSI fluorescence with the formation of $P700^+$ in their PSI preparation in which the chlorophyll/P700 ratio would be around 130. In the data shown in Fig. 4, we were not able to detect the effects of P700 oxidation level on PSI intrinsic fluorescence level.

PSI would be excited by PSII fluorescence. The ratio of the PSI fluorescence excited by PSII fluorescence ($F_{I\leftarrow F_{II}}$) to the PI fluorescence directly excited by the 460 nm light ($F_{I\,direct}$) increases with the Chl content per unit area (See Appendix and Fig. S5). Then, F_{Iv}/F_{Im} should also increase with the increase in the Chl content per area. However, this trend was not observed (Fig. 5). $F_{I\leftarrow F_{II}}/F_{I\,direct}$ may be expressed by Eq. A14 (see Appendix), which is the product of the yield of PSII fluorescence and the ratio of the integrals (see Eq. 14 in the Appendix). The former would be a few percent (Latimer et al. 1956, Lamb et al. 2018). The latter would be less than 1~2. Thus, $F_{I\leftarrow F_{II}}/F_{I\,direct}$ may be negligible.

Spillover in fluorescence quenching analyses

Fluorescence is a potent probe to analyse photosynthetic reactions. However, in many fluorescence models, spillover is not considered. Let us assume that the initial allocation of Chl*s to PSII is Ψ_{II}. Maximum quantum yield of PSII photochemistry with no energy dependent quenching (NPQ) on absorbed PFD (Φ_{II}) may be expressed as follows (Kono et al. 2024). In the present consideration, we deal with F_{II0} and F_{IIm} only. Thus, the equations used here are identical to those used by Kitajima and Butler (1975a, b).

$$\Phi_{II} = \Psi_{II} \cdot \frac{k_P}{k_P + k_F + k_D + k_{inc} + k_S} = \Psi_{II} \cdot \frac{k_P}{\sum k} \qquad \text{Eq. 1}$$

where Ψ_{II} is the share of initial allocation of Chl*s to PSII and k are the first-order rate constants: k_P, photochemistry; k_F, radiative (fluorescence) deexcitation; k_D, thermal deexcitation to the ground state via pathways other than NPQ (non-photochemical quenching); k_{isc}, intersystem crossing leading to formation of ^{T}Chl*; and k_S spillover to PSI. Let us assume F_{IIv}/F_{IIm} is 0.8. Namely,

$$k_P/\sum k = 0.8 \qquad \text{Eq. 2}$$

and

$$(k_F + k_D + k_{inc} + k_S)/\sum k = 0.2\,. \qquad \text{Eq. 3}$$

Then, for equal excitation of PSII and PSI in weak light, we may assume that Φ_{II} and Φ_I are identical:

$$0.8 \cdot \Psi_{II} = 1 - \Psi_{II} + (k_S/\sum k) \cdot \Psi_{II} \qquad \text{Eq. 4}$$

The spillover ratio ranged from 0.3 ~ 0.4 (Fig. 3):

$$\frac{F_{I\beta}}{F_{I\alpha} + F_{I\beta}} = \left(\frac{k_S}{k_F + k_D + k_{inc} + k_S} \cdot \Psi_{II}\right) / \left(1 - \Psi_{II} + \frac{k_S}{k_F + k_D + k_{inc} + k_S} \cdot \Psi_{II}\right) = 0.3 \sim 0.4. \qquad \text{Eq. 5}$$

Solving Eq. 4 and Eq. 5 simultaneously, Ψ_{II} ranges from 0.58 to 0.59 and $k_S/\sum k$ ranges from 0.063 to 0.094. When PSII reaction centres are all open, 6 to 9% Chl*s initially allocated to PSII are redirected to PSI. When all the PSII reaction centres are closed, 32 to 47% of excitations are redirected towards PSI. Although the relative contribution of spillover decreases with the increase in NPQ, it is obvious that spillover should not be neglected.

Chloroplast ultrastructure

Figs. 6 shows chloroplast structure of *A. odora* leaves. As expected, thylakoid membrane length per unit volume was greater in the chloroplasts in the LL leaf than those in the HL leaf. If we assume the thickness of thylakoids is 13 nm (Kirchhoff 2019), the thylakoids volume per unit chloroplast volume becomes 34 and 49% in HL and LL chloroplasts. It is noteworthy that the length ratios of non-appressed membranes per total thylakoid membranes were comparable between LL and HL samples. Although the grana morphology has been attracted much attention (Skene 1974, Terashima et al. 1986) and rearrangement of grana in response to light has been shown (Rozak et al. 2002, Kirchhoff 2019), detailed dynamics of the intergrana thylakoids have not been clarified. However, including extensive intergrana thylakoids, the fractions of the non-appressed thylakoid membranes were similar and more than 40% in both HL and LL chloroplasts. In the present study, we did not analyse the effects of illumination, because we are mainly interested in spillover upon sudden exposure of shaded leaves to high light. Detailed dynamics of the intergrana thylakoids should be studied.

We do not know where in the thylakoids the spillover from PSII to PSI occurs. Since it would occur in the non-appressed thylakoid membranes, it is necessary to quantify the non-appressed thylakoids. For the Förster-type transfer to occur, the set of pigments should be located close enough. For chlorophylls, the distance which allows 50% probability of energy transfer is calculated to be 5~10 nm (Van Grondelle et al. 1994), then the jump across the inter-thylakoid partition (~ 4 nm, according to Kirchihoff 2019) would be possible. Then, energy transfer may not be confined to within the same membrane. However, based on analyses of the decay time of fluorescence, it has been argued that the main pathway of the spillover is within the same membrane (Farooq et al. 2016).

It is worth pointing out that the appressed thylakoid membranes may also accommodate megacomplexes in their margins. Assuming that the size of a PSI-PSII megacomplex is 25 nm (Yokono et al. 2015, Kim et al. 2023) and the diameter

563 of the granum is 400 to 600 nm (Fig. 6 of this paper, Kirchhoff 2019) then the
564 marginal area corresponding to 23 to 16% of the disc-shaped appressed thylakoid
565 membrane may accommodate the megacomplexes. Then, the membrane area which
566 can accommodate the PSI-PSII megacomplexes approaches more than 50% in both
567 HL and LL chloroplasts.
568
569 **Conclusions and a brief ecological consideration**
570
571 The present study showed that spillover occurs in all plant materials including
572 low-light grown shade tolerant *A. odora* and the Chl *b* less mutant. The organized
573 spillover would occur within the PSI -PSII megacomplexes in the non-appressed
574 thylakoid membranes and in the marginal areas of appressed-thylakoids. It is
575 noteworthy that these parts would comprise more than 50% of the total thylakoid
576 membranes in both LL and HL-grown *A. odora*. In nature, shade tolerant species
577 are in the low light environments, mainly shaded by plants. In such green shade,
578 far-red light is enriched. Thus, the thylakoids of these plants are in State 1, and
579 operate photosynthesis at the highest efficiency without NPQ. Upon sudden
580 exposure of such leaves to high light due to sun patches (Smith and Berry 2013) or
581 sunflecks (Pearcy and Way 2012), excitations initially allocated to PSII would be
582 spilt over to PSI most efficiently. Since the decreased electron flow and increased
583 excitation flow to PSI contribute to formation of $P700^+$, the safe quencher, the
584 spillover protects both PSII and PSI from photoinhibition.
585
586

Materials and Methods

Plant Materials

Cucumis sativus L. (cucumber) "Nanshin," *Spinacia oleracea* L. (spinach) "Torai," *Alocasia odora* (G. Lodd.) Spach, and *Hordeum vulgare* L.(barley) "Gunilla, Svalöf AB N83-4001," a wild type, and *H. vulgare* "Dornaria, chlorina-f2^{2800}," a chlorophyll *b*-less mutant, were grown in vermiculite in pots in growth chambers at 25°C. Light period was 12 h. Light was provided by a bank of white fluorescent lamps. Photon flux density (PFD) levels were adjusted with the number of fluorescent tubes and/or the black shade cloth. Cucumber, spinach, and *A. odora* were grown at two photosynthetic PFD (400–700 nm) levels. For cucumber and spinach, the PFD levels were 400 and 100 µmol m^{-2} s^{-1}, while for *A. odora*, 100 and 10 µmol m^{-2} s^{-1} were used. Barley plants were grown at 400 µmol m^{-2} s^{-1}. For electron microscopy, *A. odora* grown at 180 and 10 µmol m^{-2} s^{-1} were used. Plants were given the 1/1000 strength of the Hyponex 6–10–5 solution (Hyponex, Japan) diluted with tap water every two or three days. The relative humidity of the chamber was kept above 50%.

77K fluorescence from leaf discs

Fluorescence induction at 77K was measured with a PAM 101 fluorometer (Walz, Effeltrich, Germany). The original red LED (650 nm) used for the pulse-modulated measuring light was replaced with a blue LED (OSUB5111AST, OptoSupply, Hong Kong) peaked at 460 nm. In the PAM 101 fluorometer, a photodiode was used to detect fluorescence. The original far-red filter was replaced with a 690 nm or 760 nm bandpass filter (HMX0690 or HMX0760, Asahi-Spectra, Tokyo, Japan) for PSII or PSI fluorescence measurements.

Leaf discs (10 mm in diameter) were cut with a leaf punch. 16 leaf discs were used for one series of measurements. For one set of measurements, four leaf discs were used, and fluorescence inductions were measured at 690 and 760 nm, respectively, in States 1 and 2. These four discs were taken from a narrow uniform part of a leaf. For cucumber, spinach, and *A. odora* 16 leaf discs were taken from one leaf, whereas, for barley, four sets were taken from four separate leaves. The leaf discs were placed on wet filter paper with the adaxial sides upward and illuminated with State 2 light at 470 nm from LEDs (L470, Ushio, Tokyo) or State 1 light at 720 nm from LEDs (L720, Ushio, Tokyo) at a photon flux density of 10 µmol m^{-2} s^{-1} at a room temperature of ca. 25°C. For *A. odora* leaves grown at 10 µmol m^{-2} s^{-1}, the PFD level was lowered to 5 µmol m^{-2} s^{-1}. After illumination for at least 30 min with either of the State 1 or State 2 LEDs, the adaxial side of leaf disc was attached to a quartz rod with silicone grease and covered with an aluminum cap and dipped in liquid nitrogen in a Dewer jar. All these procedures were made within 2 min in dim light (for the measurement system, see Fig. S1). When the temperature of the sample in the aluminum cap was equilibrated with the liquid nitrogen, which was detectable by a change of the sound of bubbling, recording was started. After 2 s, the measuring/actinic blue light at 50 µmol m^{-2} s^{-1} (pulse modulated at 100 kHz) was turned on. The fluorescence induction at 690 nm or 760 nm was recorded at 1 ms time intervals for 28 s on a USB data acquisition system (USB-1608FS, Measurement Computing, Norton, MA, USA).

Effects of NPQ on the spillover

The effects of NPQ on the spillover were examined using an *A. odora* leaf grown at 10 µmol m^{-2} s^{-1} light. The leaf disc attached to a quartz rod was covered with an aluminum cap, and NPQ was induced by illuminating the leaf disc with an actinic white light from a tungsten lamp (KL1500 lcd, Schott, Mainz, Germany) at 700 µmol m^{-2} s^{-1} for 270 s at a room temperature of ca. 23℃. Saturating flashes at 6,600 µmol m^{-2} s^{-1} for 1 s were given at 20 s intervals. The actinic light was

turned off, and 10 s after, the measuring beam was turned off. At 5 s after turning off the actinic light, far-red light peaked at 720 nm at 10 μmol m^{-2} s^{-1} was illuminated for 10 s to oxidize PSII. Then, the leaf disc in the cap was frozen at 77K. When the temperature reached 77K, PSI or PSII fluorescence was measured as above.

Effects of $P700^+$ formation on PSI fluorescence

PSI fluorescence was obtained by preferential illumination of PSI pigments. The actinic/measuring light was a 700 nm LED (5 mm bullet type, Ushio, Tokyo, Japan) passing through a 700 nm band pass filter with 10 nm half-band width (HMX700, Asahi-spectra, Tokyo, Japan) and a 710 nm short pass filter (SVX 710). For detection of PSI fluorescence, the photodiode of the PAM 101 covered with a long pass filter (LVX 730, allowing transmission of far-red light > 730 nm) was used. Since it was necessary to use the measuring/actinic light of very narrow waveband, the PFD level at the leaf disc surface was 0.07 μmol m^{-2} s^{-1}.

The leaf disc kept in the dark at least for 30 min was attached to the quartz rod, enclosed by an aluminum cup, chilled at 77 K, and its PSI fluorescence was measured. The accumulation of $P700^+$ was measured with a dual-wavelength (820/870 nm) unit (ED-P700DW) attached to a PAM fluorometer (Walz) in the reflectance mode. When the two PAM101 systems were operated at the same time, the signals sometimes became noisy. Thus, we used similar leaf discs taken from the same leaf and measured the PSI fluorescence and redox state of P700 separately, but according to the same illumination time schedule.

After the onset of recording at 4 ms intervals, the measuring/actinic light for PSI at 0.07 μmol m^{-2} s^{-1} was on at 15 s. The signal damping was started to reduce the noise level at 30 s, an unmodulated blue light at 58 μmol m^{-2} s^{-1} was added at 60 s, the blue light level was increased to 360 μmol m^{-2} s^{-1} at 80 s, and, the blue light was turned off and a white light from a tungsten lamp at 3000 μmol m^{-2} s^{-1} was turned on at 100 s. When the redox state of P700 was measured, the pulse-modulated measuring light from a PAM 101 far-red LED emitting light with wavelengths ranging from 800 to 900 nm was used, in addition to the lighting protocol including the PSI measuring/actinic light as mentioned above.

Effects of excitation of PSI fluorescence by re-absorbed PSII fluorescence

To examine the effects of chlorophyll concentrations on PSI fluorescence excited by reabsorbed PSII fluorescence, thylakoids were prepared from spinach as described in Terashima et al. (2021). PSI fluorescence induction in the thylakoid suspension in a buffer containing 0.3 M sorbitol, 10 mM NaCl, 5 mM $MgCl_2$ and 50 mM and Hepes-KOH (pH at 8.0) was measured at 77K in a 3 mm thick aluminum cuvette (see Fig. S1). All these procedures were made in dim light. The pulse modulated measuring/excitation light at 460 nm used was at the PFD of 12 μmol m^{-2} s^{-1}. The weaker light was used to obtain more data points for the induction phase with the diluted thylakoid suspensions. For theoretical consideration, see the supplementary material.

Data processing

F_0 and F_m determination for leaf discs: The recording system was turned on at 0 s, and the measuring/actinic light was turned on at 2 s. The zero (0) and the maximum fluorescence (F_m) levels were obtained by averaging 2000 data points between 0 and 2 s and between 28 s and 30 s. A linear regression line was obtained for the 50 data points, from 2.005 to 2.054 s, and the value at 2 s was regarded as F_0.

F_m and F_0 thus obtained were used to calculate F_v (= $F_m - F_0$), and F_v / F_m. As the increases in PSI and PSII fluorescence intensities were synchronized (Fig. 1), the variable fluorescence in PSI was assumed to be attributed to the spillover from

PSII variable fluorescence.

The spillover from PSII to PSI was assumed to occur at the same efficiency even when the PSII fluorescence was F_0, according to Strasser and Butler (1977a, b). Based on these assumptions, PSI fluorescence at time t, $F_{\mathrm{I}}(t)$, was expressed as:

$$F_{\mathrm{I}}(t) = F_{\mathrm{I}\alpha} + \beta \cdot F_{\mathrm{II}}(t). \qquad \text{Eq. 6}$$

From this, intrinsic PSI fluorescence ($F_{\mathrm{I}\alpha}$) was obtained:

$$F_{\mathrm{I}\alpha} = F_{\mathrm{I}m} - (F_{\mathrm{I}m} - F_{\mathrm{I}0}) \cdot \frac{F_{\mathrm{II}m}}{F_{\mathrm{II}m} - F_{\mathrm{II}0}}. \qquad \text{Eq. 7}$$

Induction time determination: Assuming that the PSII fluorescence induction occurred in two phases, the induction curve was fitted by the equation:

$$F(t) = F_0 + \cdot a \cdot [1 - exp(-k_1 \cdot t)] + (F_m - F_0 - a) \cdot [1 - exp(-k_2 \cdot t)] \qquad \text{Eq. 8}$$

We used F_0 and F_m, which were obtained as above. A, k_1 and k_2 were obtained by the fitting with KaleidaGraph (Version 5.0, Synergy Software). Then, $t_{1/2}$ was obtained as t giving $F_{\mathrm{II}}(t) = F_0 + (F_m - F_0)/2$.

F_0 determination for thylakoid suspension: Since a weaker actinic/measuring light was used for thylakoid suspensions, the linear regression of 50 data points was not reliable due to the lower S/N ratio. When the number of data points was simply increased, linearity could not be assumed. Thus, we fitted Eq. 8 to the fluorescence transient for 2 s to obtain F_0, a, k_1 and k_2. Because time constants k_2 was always one order of magnitude smaller than k_1, we further assumed that $k_2 = 0.1 \cdot k_1$. The determination coefficients obtained with this assumption was always greater than that for the equation in which k_1 and k_2 were independently obtained.

Electron microscopy

The *A. odora* plants used were grown at 180 or 10 μmol m^{-2} s^{-1}. After harvesting, the leaves were kept in the dark at a room temperature for at least 30 min before fixation. Leaf segments, ca. 1 mm x 4 mm were excised and fixed immediately in 2% glutaraldehyde in 0.05 M potassium phosphate buffer (pH 6.8) and kept at the room temperature for 2 h and then at 4°C overnight. Six rinses in the buffer solution preceded postfixation with 2% OsO_4 in the buffer at room temperature for 2 h. After dehydration in a graded acetone series, leaf materials were embedded in Spurr's resin. The ultrathin sections (silver-gold) were poststained with uranyl acetate and lead citrate and examined with a Hitachi H-7500 transmission electron microscope at an accelerating voltage of 80 kV.

Electron-micrographs of the first cell layers of the palisade tissues were taken to avoid the effects of intra-leaf light gradient on thylakoid morphologies (Skene 1974, Terashima et al. 1986, Terashima and Hikosaka 1995). In the leaves grown at 180 or 10 μmol m^{-2} s^{-1} light, 36 or 30 chloroplasts were randomly chosen, and in these chloroplasts, 178 or 157 squares of 1 μm^2, in which all thylakoid membranes were in focus, were selected randomly. We randomly selected 10 of these squares from 10 chloroplasts for each growth light level and thylakoid lengths were measured using Fiji/ImageJ (NIH).

The total length of the thylakoid membranes per 1 μm^2 was also calculated as an index of thylakoids to stroma volume ratio. The abundance of non-appressed thylakoids was expressed as the ratio of the length of the non-appressed thylakoid membranes to the total thylakoid membranes.

Funding

This work was partly supported by grants from Japan Society for the Promotion of Science (17H05718, 19H04718, 22H02640 and 23K23903).

Acknowledgement

The barley seeds were a kind gift of Professor WS Chow, The Australian National University. We thank Dr. Masao Kitajima for valuable inputs. We also thank Dr. G. Shansker for drawing our attention to PSI fluorescence excited by PSII fluorescence. Mr. Hashimoto, and Mr. Okamoto, A. from Namoto Co., Ltd. for assisting modification the optical system of the PAM 101.

Author Contributions

All authors contributed to this study and are responsible for the content of this paper. All authors have no conflicts of interests.

Disclosure

The authors have no conflict of interest.

Supplementary Figures

Fig. S1: The optics and cuvettes for fluorescence measurements.
Fig. S2: Relationships between PSII and PSI fluorescence.
Fig. S3: Determination of *absorption coefficients by curve fitting*.
Fig. S4: The ratio of the integrations in Eq. A10 as a function of the Chl content.
Fig. S5: Estimation of the absorption coefficient of PSII fluorescence.
Fig. S6: The measurements of total thylakoid membrane length.

References

Akhtar, P., Balog-Vig, F., Han, W., Li, X., Han, G., Shen, J.-R., Lambrev, P.H. (2024) Quantifying the energy spillover between photosystem II and I in cyanobacterial thylakoid membranes and cells. Plant Cell Physiol. 65: 95-106.

Anderson, J.M. (1986) Photoregulation of the composition, function, and structure of thylakoid membranes. Annu. Rev. Plant Physiol. 37: 93-136.

Anderson, J.M. and Andersson, B. (1988) The dynamic photosynthetic membrane and regulation of solar energy conversion. Trend. Biochem. Sci. 13: 351-355.

Bag, P., Chukhutsina, V., Zhang,Z., Paul, S., Ivanov, A.G., Shutova1, T., Croce, R., Holzwarth, A.R., and Jansson, S (2020) Direct energy transfer from photosystem II tophotosystem I confers winter sustainability in Scots Pine. Nat. Comm. 11: 6388. https://doi.org/10.1038/s41467-020-20137-9

Bassi, R. and Dall'Osto, L. (2021) Dissipation of light energy absorbed in excess: The molecular mechanisms. Annu. Rev. Plant Biol. 72: 47-76.

Bellaflore, S., Barneche, F., Peltler, G. and Rochaix, J.D. (2005) State transitions and light adaptation require chloroplast thylakoid protein kinase STN7. Nature 433: 892-895.

Björkman. O. (1981) Responses to different quantum flux densities. In: Lange, O.K., Nobel, P.S., Osmond, C.B. and Ziegler, H. (eds) Encyclopedia of Plant Physiology, New Series, vol 12A. Springer, Berlin, pp 57–106.

Blankenship, R.E. (2021) Molecular Mechanisms of Photosynthesis. 3rd edn. P. 328. Wiley, Hoboken.

Chow, W.S., Qian, L., Goodchild, D.J. and Anderson, J.M. (1988) Photosynthetic acclimation of *Alocasia macrorrhiza* (L.) G. Don. Aust. J. Plant Physiol. 15:107–122. https:// doi. org/ 10. 1071/ PP988 0107

Demmig-Adams, B. and Adams III, WW. (2006) Photoprotection in an ecological context: The remarkable complexity of thermal energy dissipation. New Phytol. 172: 11-21.

Evans J.R. and Anderson, J.M. (1987) Absolute absorption and relative fluorescence

827 excitation spectra of the five major chlorophyll-protein complexes from spinach
828 thylakoid membranes. Biochim. Biophys. Acta 892: 75-82.
829
830 Farooq, S., Chmeliov, J., Trinkunas, G., Valkunas, L. and van Amerongen, H. (2016)
831 Is there excitation energy transfer between different layers of stacked photosystem-
832 II-con-taining thylakoid membranes? J. Phys. Chem. Lett. 7: 1406–1410. https://
833 doi.org/10.1021/acs.jpclett.6b00474.
834
835 Franck, F., Juneau P., and Popovic, R. (2002) Resolution of the Photosystem I and
836 Photosystem II contributions to chlorophyll fluorescence of intact leaves at room
837 temperature. Biochim Biophys.Acta 1556: 239-246.
838
839 Garcia-Molina, A. and Leister, D. 2020 Accelerated relaxation of photoprotection
840 impairs biomass accumulation in *Arabidopsis*. Nat. Plant 6: 9-12.
841
842 Girolomonia, L., Cazzanigaa, S., Pinnola, A., Perozenia, F., Ballottaria, M. and
843 Bassi, R. (2019) LHCSR3 is a nonphotochemical quencher of both photosystems in
844 *Chlamydomonas reinhardtii*. Proc. Natl. Acad. Sci. USA. 116: 4212-4217.
845
846 Grieco, M., Tikkanen, M., Paakkarinen, V., Kangasjärvi, S. and Aro, E.M. (2012)
847 Steady-state phosphorylation of light-harvesting complex II proteins preserves
848 photosystem I under fluctuating white light. Plant Physiol. 160: 1896-1910.
849
850 Horton, P. and Lee, P. (1985) Phosphorylation of chloroplast membrane proteins
851 partially protects against photoinhibition. *Planta* 165: 37-42.
852
853 Ifuku, K. (2023) Diversity of the PSI–PSII megacomplexes that conduct energy
854 spillover in green plants. Plant Cell Physiol. 64: 844-846.
855 doi:https://doi.org/10.1093/pcp/pcad069,
856
857 Ikegami, I. 1976 Fluorescence changes related in the primary photochemical
858 reaction in the P-700-enriched particles isolated from spinach chloroplasts.
859 Biochim. Biophys. Acta 449: 245-258.
860
861 Inoue, Y., Ogawa, T. and Shibata, K. (1973) Light-induced spectral changes of P700
862 in the 800-nm region in *Anacystis* and spinach lamellae. Biochim. Biophys. Acta
863 305: 483-487.
864

Kasahara, M., Kagawa, T., Oikawa K., Suetsugu, N., Miyao, M. and Wada, M. (2002) Chloroplast avoidance movement reduces photodamage in plants. Nature 420: 829-832.

Khorobrykh, S., Havurinne, V., Mattila, H. and Tyystjärvi, E. (2020) Oxygen and ROS in photosynthesis. Plants 9: 91 doi:10.3390/plants9010091

Kim, E., Yokono, M., Tsugane, T., Ishii, A., Noda, C. and Minagawa, J. (2023) Formation of a stable PSI–PSII megacomplex in rice that conducts energy spillover. Plant Cell Physiol. 64: 858-865. https://doi.org/10.1093/pcp/pcad037

Kirchhoff, H. 2019 Chloroplast ultrastructure in plants. New Phytol. 223: 565-574.

Kitajima, M., Butler, W.L. (1975a) Quenching of chlorophyll fluorescence and primary photochemistry in chloroplasts by dibromothymoquinone. Biochim. Biophys. Acta 376:105–115.

Kitajima, M., Butler, W.L. (1975b) Excitation spectra for photosystem I and photosystem II in chloroplasts and the spectral characteristics of the distribution of quanta between the two photosystems. Biochim. Biophys. Acta 408:297–305.

Kono, M., Kawaguchi, H., Mizusawa, N., Yamori, W., Suzuki, Y. and Terashima, I. (2020) Far-red light accelerates photosynthesis in the low-light phases of fluctuating light. Plant Cell Physiol. 61: 192–202. https://doi.org/10.1093/pcp/pcz191

Kono, M., Oguchi, R. and Terashima, I. (2024) Photoinhibition of PSI and PSII in nature and in the laboratory: Ecological approaches. Prog. Bot. 84: 241–292. https://doi.org/10.1007/124_2022_67

Kromdijk., J., Głowacka, K., Leonelli, L., Gabilly, S.T., Iwai, M., Niyogi, K.K. and Long, S.P. (2016) Improving photosynthesis and crop productivity by accelerating recovery from photoprotection. Science 354: 857-861. 10.1126/science.aai8878

Lamb, J.J., Røkke, G. and Hohmann-Marriot, M.F. 2018 Chlorophyll fluorescence emission spectroscopy of oxygenic organisms at 77 K. Photosynthetica 56: 105-124.

Latimer, P., Bannister, T.T. and Rabinowitch, E. (1956) Quantum yields of fluorescence of plant pigments. Sicnece 124: 585-586.

Miyake, C. (2020) Molecular mechanisms of oxidation of P700 and suppression of

905 ROS production in photosystem I in response to electron-sink limitations in C3
906 plants. Antioxidants 9:230. https://doi.org/10.3390/antiox9030.230
907
908 Murata, N. (1969) Control of excitation transfer in photosynthesis. I. Light-induced
909 change of chlorophyll a fluorescence in *Porphyridium cruentum*. Biochim. Biophys.
910 Acta 172: 242-251.

911 Pastenes, C., Pimentel, P. and Lillo, J. 2005 Leaf movements and photoinhibition
912 in relation to water stress in field-grown beans. J. Exp. Bot. 56: 425-433.

913 Pearcy R.W. (1990) Sunflecks and photosynthesis in plant canopies. Annu. Rev.
914 Plant Physiol. Plant Mol. Biol. 41: 421-453.

915 Pursiheimo, S., Rintamäki, E., Baena-Gonzalez, E. and Aro, E.M. (1998) Thylakoid
916 protein phosphorylation in evolutionally divergent specieswith oxygenic
917 photosynthesis FEBS Lett. 423: 178-182.
918
919 Rintamäki, E., Salonen, M., Suoranta, U.-M., Carlberg, I., Andersson, B. and Aro,
920 E.M. 1997, Phosphorylation of light-harvesting complex II and photosystem II core
921 proteins shows different irradiance-dependent regulation in vivo. J. Biol. Chem.
922 272: 30476-30482.
923
924 Rozak, P.R., Seiser, R.M., Wacholtz, W.F. and Wise, R.R. (2002) Rapid, reversible
925 alterations in spinach thylakoid appression upon changes in light intensity. Plant
926 Cell Environ. 25: 421-429.
927
928 Ruban, A.V., Johnson, M.P., Duffy, C.D.P. (2012) The photoprotective molecular
929 switch in the photosystem II antenna. Biochim. Biophys. Acta 1817: 167-181.
930
931 Schlodder, E., Çetin, M., Byrdin, M., Terekhovac, I.V. and Karapetyan, N.V. (2005)
932 $P700^{+}$- and $^{3}P700$-induced quenching of the fluorescence at 760 nm in trimeric
933 Photosystem I complexes from the cyanobacterium *Arthrospira platensis*. Biochim.
934 Biophys. Acta 1706: 53-67. doi:10.1016/j.bbabio.2004.08.009
935
936 Skene, D. S. (1974) Chloroplast structure in mature apple leaves grown under
937 different levels of illumination and their response to changed illumination. Proc. R.
938 Soc. London B 186: 75-78.
939

940 Smith, W.K. and Berry Z.C. (2013) Sunflecks? Tree Physiol. 33：233-237.

941

942 Strasser, R. and Butler, W.L. (1977a) Energy transfer and the distribution of
943 excitation energy in the photosynthetic apparatus of spinach choiroplasts. Biochim.
944 Biophys. Acta 460: 230-238.
945
946 Strasser, R. and Butler, W.L. (1977b) The yield of energy transfer and the spectral
947 distribution of excitation energy in the photochemical apparatus of flashed bean
948 leaves. Biochim. Biophys. Acta 462: 295-306.
949
950 Terashima, I., Hikosaka, K. (1995) Comparative ecophysiology of leaf and canopy
951 photosynthesis. Plant Cell Environ. 18:1111–1128
952
953 Terashima, I., Matsuo, M., Suzuki, Y., Yamori, W. and Kono, M. (2021)
954 Photosystem I in low light-grown leaves of *Alocasia odora*, a shade-tolerant plant,
955 is resistant to fluctuating light-induced photoinhibition. Photosynth. Res. 149:69–
956 82.
957
958 Terashima, I., Sakaguchi, S. and Hara, N. (1986) Intra-leaf and intercellular
959 gradients in chloroplast ultrastructure of dorsiventral leaves illuminated from the
960 adaxial or abaxial side during their development. Plant. Cell Physiol. 27: 1023-
961 1031.
962
963 Tokutsu, R., and J. Minagawa. (2013). Energy-dissipative supercomplex of
964 photosystem II associated with LHCSR3 in *Chlamydomonas reinhardtii*. Proc. Natl.
965 Acad. Sci. USA 110: 10016-10021
966
967 Trrisl, H.-W., Breton, J., Deprez, J. and Leibl, W. (1987) Primary electrogenic
968 reactions of photosystem II as probed by the light-gradient method. Biochim
969 Biophys Acta 893: 305-319.
970
971 Van Grondelle, T., Dekker, J.P., Gillbro, T. and Sundstrom V. (1994) Energy transfer
972 and trapping in photosynthesis. Biochim. Biophys. Acta 1187: 1-65.
973
974 Weis, E. (1985) Light-and temperature-induced changes in the distribution of
975 excitation energy between Photosystem I and Photosystem II in spinach leaves.
976 Biochim. Biophys. Acta 807: 118-126.
977
978 Wientjes, E. and Croce, R. (2012) PMS: Photosystem I electron donor or
979 fluorescence quencher. Photosynth. Res. 111: 185-191.
980
981 Yokono, M., Takabayashi, A., Akimoto, S. and Tanaka, A. (2015) A megacomplex
982 composed of both photosystem reaction centres in higher plants. Nat. Comm. 6:

983 6675. DOI: 10.1038/ncomms7675
984
985 Yokono, M., Takabayashi, A., Kishimoto, J., Fujita, T., Iwai, M., Murakami, A.,
986 Akimoto, S. and Tanaka, A. (2019) The PSI–PSII megacomplex in green plants.
987 Plant Cell Physiol. 60: 1098-1108.
988
989

Table 1. Chl content, Chl a/b, F_{IIv}/F_{IIm} and $t_{1/2}$ of PSII fluorescence induction.

	Growth light (μmol m^{-2} s^{-1})	Chl (mmol m^{-2})		Chl a/b		State	F_{IIv}/F_{IIm}		$t_{1/2}$			
		mean ± sd	P	mean ± sd	P		mean ± sd	P	mean ± sd	P	P (HL vs. LL)	
											State 1	State 2
Cucumis sativus	400	0.26± 0.024	*0.607*	5.08 ± 0.141	***1.54E-05***	1	0.850 ± 0.018	*0.32*	0.336 ± 0.017	*0.652*	***0.000564***	
						2	0.836 ± 0.019		0.344 ± 0.030			***0.00855***
	150	0.25 ± 0.028		4.06 ± 0.080		1	0.824 ± 0.005	*0.897*	0.255 ± 0.017			
						2	0.823 ± 0.014		0.279 ± 0.016	*0.0886*		
Spinacia oleracea	400	0.62 ± 0.048	***0.00447***	3.86 ± 0.073	***0.00554***	1	0.781 ± 0.033	*0.52*	0.319 ± 0.055	*0.551*	***0.0626***	
						2	0.794 ± 0.019		0.338± 0.020			*0.246*
	150	0.49 ± 0.034		3.59 ± 0.105		1	0.777 ± 0.042	*0.5135*	0.251 ± 0.023			
						2	0.793 ± 0.019		0.307± 0.040	***0.053***		
Alocasia odora	100	0.63 ± 0.024	***0.005431***	3.96 ± 0.025	***1.70E-06***	1	0.851 ± 0.006	***0.0016***	0.353 ± 0.013		***0.00395***	
						2	0.810 ± 0.014		0.377 ± 0.046	*0.36*		*0.105*
	10	0.54 ± 0.035		3.52 ± 0.041		1	0.774 ± 0.015	*0.264*	0.286 ± 0.026			
						2	0.755 ± 0.027		0.326 ± 0.026	***0.0724***		
Hordeum vulgare WT	400	0.38 ± 0.068	***0.00156***	3.75 ± 0.194		1	0.822 ± 0.028	*0.203*	0.338 ± 0.029			
						2	0.797 ± 0.021		0.493 ± 0.030	***0.000294***		
Chl *b*-less mutant	400	0.18 ± 0.027		>>		1	0.731 ± 0.059	*0.277*	1.259 ± 0.080	*0.194*		
						2	0.694 ± 0.017		1.348 ± 0.093			

Each of the data is shown as the mean ± S.D. (n = 4). Student's t test was used to detect statistical differences. When P <0.1, P values are shown in bold by the higher values. Chl a/b ratio in the Chl b-less barley was not determined and was noted by >>.

Table 2. PSI fluorescence properties

	Growth light (μmol m^{-2} s^{-1})	State	F_{IIm}		$F_{I\alpha}$		F_{Im}		F_{Iv}/F_{Im}	
			mean ± sd	*P*	mean ± sd	*P*	mean ± sd	*P*	mean ± sd	*P*
Cucumis sativus	400	1	1.58 ± 0.075	***0.005***	1.09 ± 0.059		1.63 ± 0.058		0.319 ± 0.008	***0.00096***
		2	1.41 ± 0.027		1.32 ± 0.063	***0.0017***	1.87 ± 0.075	***0.0026***	0.290 ± 0.006	
	150	1	1.73 ± 0.036	***0.0048***	0.71 ± 0.028		1.15 ± 0.053	*0.56*	0.316 ± 0.009	***0.003***
		2	1.54 ± 0.079		0.78 ± 0.050	***0.048***	1.18 ± 0.053		0.277 ± 0.014	
Spinacia oleracea	400	1	1.49 ± 0.146	***0.06***	0.59 ± 0.098		0.95 ± 0.135	*0.188*	0.299 ± 0.029	***0.0087***
		2	1.30 ± 0.082		0.77 ± 0.063	***0.027***	1.08 ± 0.098		0.238± 0.012	
	150	1	2.15 ± 0.150	***0.0028***	0.83 ± 0.091	*0.25*	1.35 ± 0.103	*0.93*	0.297 ± 0.016	***0.0021***
		2	1.75 ± 0.076		0.90 ± 0.055		1.30 ± 0.052		0.244 ± 0.017	
Alocasia odora	100	1	1.40 ± 0.030	***0.06***	1.00 ± 0.077	*0.49*	1.40 ± 0.077	*0.33*	0.246 ± 0.018	***0.0025***
		2	1.09 ± 0.056		1.03 ± 0.030		1.36 ± 0.034		0.202 ± 0.009	
	10	1	1.68 ± 0.084	***0.02***	1.10 ± 0.050		1.67 ± 0.071	*0.72*	0.265 ± 0.012	***0.003***
		2	1.49 ± 0.082		1.19 ± 0.045	***0.039***	1.69 ± 0.057		0.244 ± 0.017	
Hordeum vulgare WT	400	1	1.54 ± 0.119	***0.0086***	1.09 ± 0.059		1.63 ± 0.058		0.274 ± 0.025	***0.023***
		2	1.30 ± 0.050		1.32 ± 0.063	***0.0018***	1.87 ± 0.075	***0.003***	0.232 ± 0.009	
Chl *b*-less mutant	400	1	0.41 ± 0.070	*0.56*	0.33 ± 0.054	*0.84*	0.49 ± 0.092	*0.89*	0.238 ± 0.010	*0.15*
		2	0.44 ± 0.062		0.34 ± 0.079		0.51 ± 0.107		0.226 ± 0.007	

Each of the data is shown as the mean ± S.D. (n = 4). Student's *t* test was used to detect statistical differences. When $P < 0.1$, *P* values are shown in bold by the higher values.

1007 Table 3. NPQ values and F_v/F_m of PSI and PSII fluorescence inductions

1008

	NPQ	
690 nm	1.345 ± 0.0896	*0.145*
760 nm	1.220 ± 0.1192	

	F_v/F_m			
	PSII		PSI	
DARK	0.810 ± 0.0137	***0.00019***	0.241 ± 0.0120	***2.7E-05***
NPQ	0.774 ± 0.0086		0.152 ± 0.0100	

1009

1010 Each of the data is shown as the mean ± S.D. (n = 4). *P* values of the Student's *t*-tests
1011 are shown.

1012
1013
1014
1015

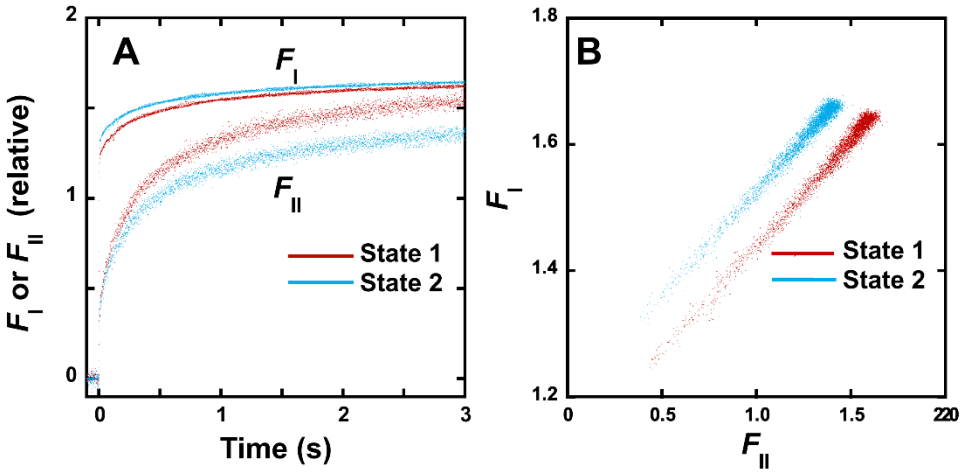

Fig. 1. Induction curves of PSI and PSII fluorescence and the relationships between PSI and PSII fluorescence.

A, PSI fluorescence (F_I) and PSII fluorescence (F_{II}) induction measured at 690 nm and 760 nm, respectively, in leaf discs at 77K of low light grown *Alocasia odora*. Leaf discs were illuminated with PSI light at 720 nm inducing State 1 or PSII light at 470 nm inducing State2, at the PFD of 5 µmol m^{-2} s^{-1}, for at least 30 min and frozen in liquid N_2. The fluorescence induction by the measuring/actinic light from a 460 nm LED pulse-modulated at 100 kHz was recorded. The PFD level of the measuring/actinic light at the leaf disc was 50 µmol m^{-2} s^{-1}. B, F_I plotted against F_{II}.

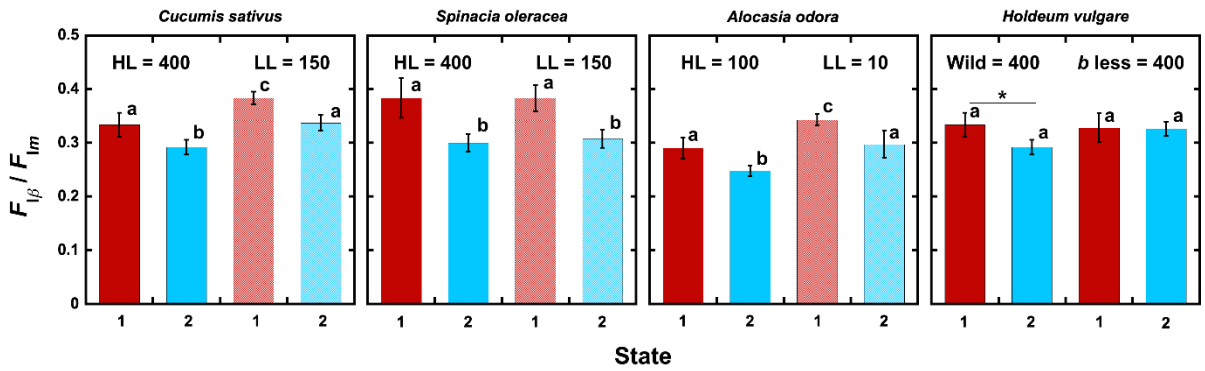

Fig. 2. Spillover ratio ($F_{I\beta}/F_{Im}$) in leaf discs in State 1 and 2.

1 and 2 on the abscissa denote State 1 and State 2, induced by PSI and PSII light at 10 µmol m^{-2} s^{-1} at least for 30 min. For LL- *A. odora*, PSI or PSII light was at 5 µmol m^{-2} s^{-1}. HL and LL denote high and low growth light. 400, 150, 100, and 10 denote photosynthetic PFD levels in µmol m^{-2} s^{-1}. Different alphabets denote statistically significant differences ($P < 0.05$) by ANOVA (Tukey-Kramer test). For HL- and LL- *H. vulgare*, *t*-test was used (* denotes $P < 0.05$).

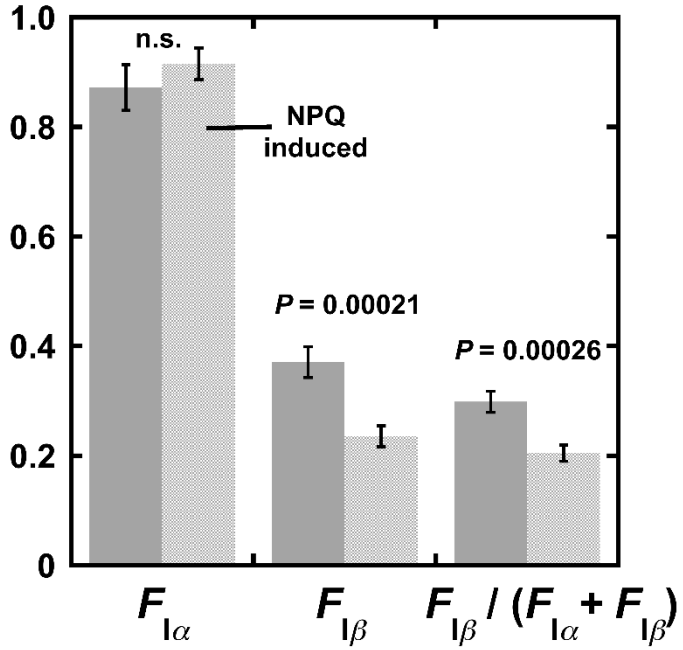

Fig. 3. Effects of NPQ induction on spillover of excitations from PSII to PSI in leaf discs from LL-grown *A. odora*.

Leaf discs from *A. odora* plants grown at 10 µmol m^{-2} s^{-1} were illuminated with an tungsten lamp at 700 µmol m^{-2} s^{-1} for 270 s and then illuminated with a 720 nm LED at 5 µmol m^{-2} s^{-1} for 10 s to oxidise the plastoquinone pool, and frozen. PSI and PSII fluorescence inductions were measured. For the control, leaf discs treated in the dark and illuminated with the 720 nm LED at 5 µmol m^{-2} s^{-1} for 10 s were used. *P* levels by *t*-test are shown.

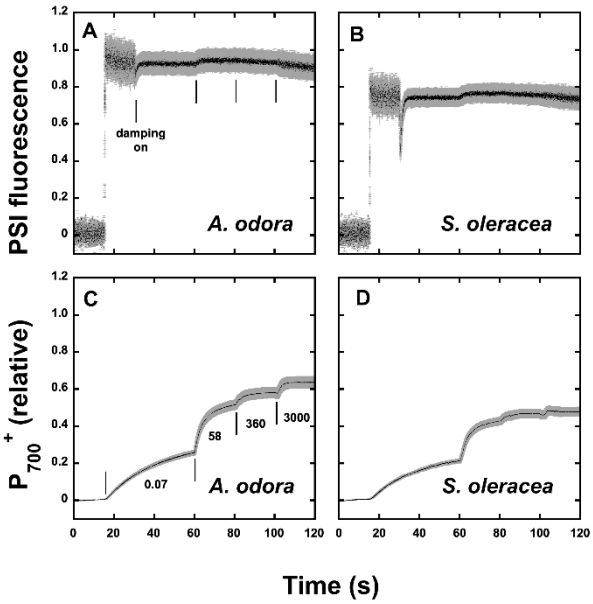

Fig. 4. PSI intrinsic fluorescence and P700^{+} formation.

A and B, Induction of PSI intrinsic fluorescence excited at 700 nm and measured in the waveband > 730 nm in the leaf discs form *A. odora* grown at 10 µmol m^{-2} s^{-1} (A) and from spinach grown at 400 µmol m^{-2} s^{-1} (B). C and D, Formation of P700^{+} in response to 700 nm light at 0.07 µmol m^{-2} s^{-1}, 470 nm blue light at 58 and 360 µmol m^{-2} s^{-1}, and white incandescent light at 3000 µmol m^{-2} s^{-1}.

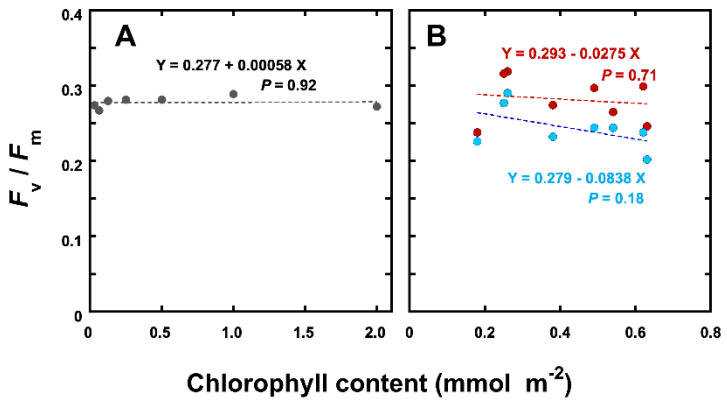

Fig. 5. F_{Iv}/F_{mv} plotted against the chlorophyll concentration in the spinach thylakoid suspension (A) and in the leaf discs used for Fig. 2 (B). Symbols in red denote State 1 data, while those in light blue denote State 2 data. Equations denote the linear regression lines with the determination coefficients with *P* values.

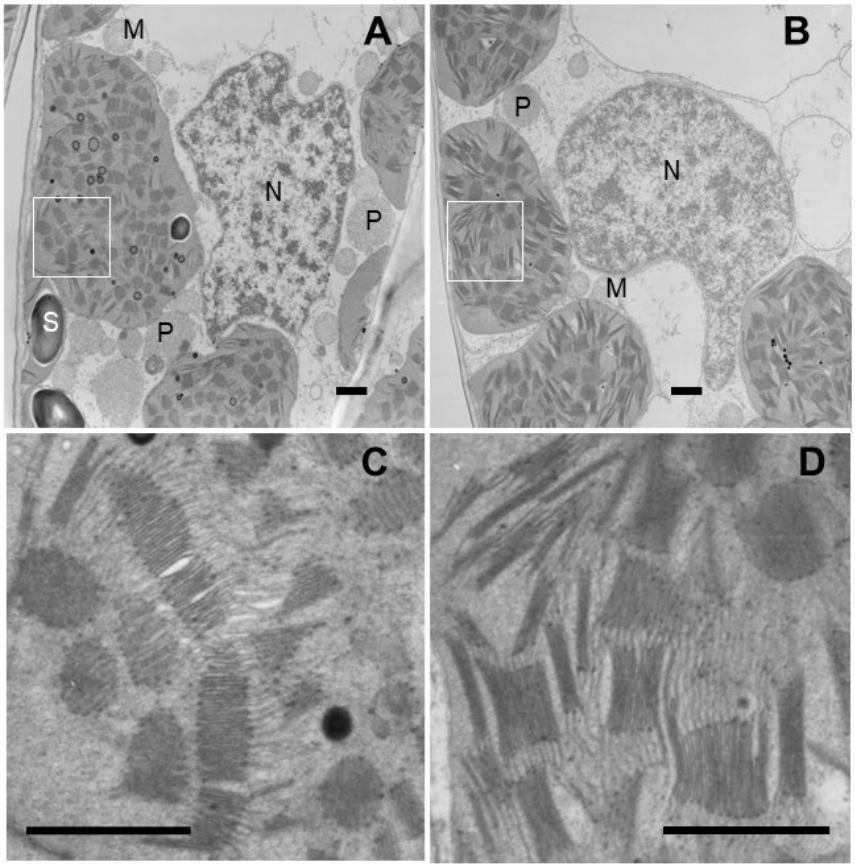

Fig. 6. Portions of the palisade tissue cells of *A. odora* leaves grown at high light (A and C) and low light (B and D). Here, high light and low light denote 180 and 10 μmol m^{-2} s^{-1}.

Near the well-developed chloroplasts, peroxisomes (P) and mitochondria (M) are observed in both samples (A and B). The square parts in A and B are enlarged in C and D. Starch grains (S) and lipid components (platoglobules) are more conspicuous in HL chloroplasts (A) than in LL chloroplasts (B). There are abundant non-appressed thylakoid membranes extending from grana stacks. Bars indicate 1 μm. SThe non-appressed thylakoid membranes / total thylakoid membranes in the central parts of these chloroplasts were 0.42 and 0.41 (See Fig. S6 A and B).

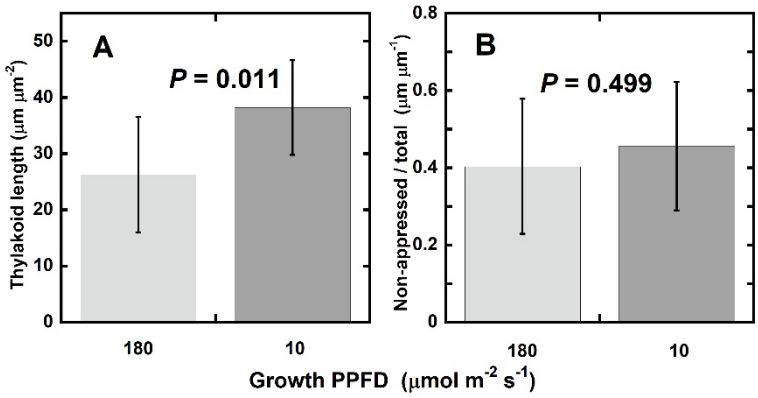

Fig. 7. Total length of thylakoid membranes per 1 μm^2 area (A) and the ratios of the total length of non-appressed thylakoid membranes to that of total thylakoid membranes (B). On electron micrographs of chloroplasts, 1 μm^2 squares in which all the thylakoid membranes were in focus were chosen, and the morphometry data, total thylakoid membrane length (A) and the ratio of the total length of non-appressed thylakoid membranes to that of total thylakoid membranes (B) were obtained for leaf segments from an *A. odora* leaf grown at 180 μmol m^{-2} s^{-1} and that grown at 10 μmol m^{-2} s^{-1}. The bar shows the mean for 10 squares (1 μm^2) from 10 different chloroplasts ± SD.

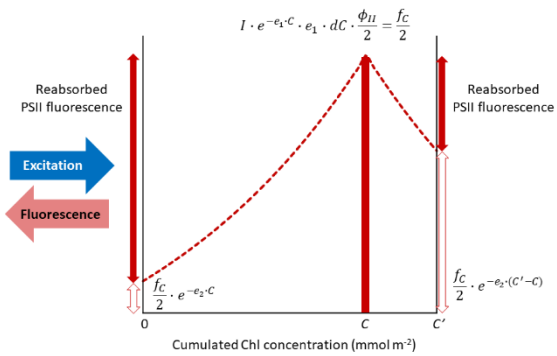

Fig. 8 A model leaf for estimation of PSI fluorescence excited by re-absorbed PSII fluorescence.

C' denotes chlorophyll content per area in mol m^{-2}. PSII fluorescence is excited by the light absorbed by *dC* at *C*. PSII fluorescence reabsorbed by the leaf can be calculated. Assuming that PSI fluorescence is not reabsorbed, we may be able estimate PSI fluorescence excited by PSII. PSII fluorescence reaching the surface can be also calculated.

APPENDIX PSI fluorescence excited by reabsorbed PSII fluorescence

Light transmission through a pigment solution in a cuvette can be expressed by the Lambert-Beer's law:

$$-\log_{10}\frac{I_t}{I_0} = \varepsilon \cdot c \cdot l \qquad \text{Eq. A1}$$

where I_0 and I_t are intensities of the incident light and transmitted light, l is the cuvette thickness, ε is an absorption coefficient, and c is the pigment concentration. Here, we consider the cumulated pigment concentration C in mol m^{-2}:

$$C = c \cdot l \qquad \text{Eq. A2}$$

Using a simple model, we consider PSI fluorescence directly excited by the measuring/actinic light and that excited by PS II fluorescence (see Fig. 8). Consider a thin layer (dC) at the cumulated chlorophyll concentration of C from the surface. Light absorption by this thin layer (dA) can be written as:

$$dA = I \cdot e^{-e_1 C} \cdot e_1 \cdot dC \qquad \text{Eq. A3}$$

where e_1 is equal to $2.30 \cdot \varepsilon_1$ and ε_1 is the absorption coefficient of Chl a+b at 460 nm (in m^2 mol^{-1}). Note that $\log_e 10 = 2.30$. PSII fluorescence emitted by this thin layer can be expressed as:

$$dF_{\mathrm{II}} = \phi_{\mathrm{II}} \cdot I \cdot e^{-e_1 \cdot C} \cdot e_1 \cdot dC \qquad \text{Eq. A4}$$

where ϕ_{II} denote PSII fluorescence yield.

Since PSII fluorescence emitted by a thin layer dC is absorbed by both sides of the layer, PSII fluorescence re-absorbed in a leaf or solution ($0 < X < C'$) can be expressed as:

$$dA = I \cdot e^{-e_1 \cdot C} \cdot e_1 \cdot dC \cdot \frac{\phi_{\mathrm{II}}}{2} \cdot [(1 - e^{-e_2 \cdot C}) + (1 - e^{-e_2 \cdot (C' - C)})] \qquad \text{Eq. A5}$$

where e_2 ($= 2.30 \cdot \varepsilon_2$) and ε_2 *is* the absorption coefficient of chlorophyll a+b at PSII fluorescence peak (~690 nm). PSI fluorescence excited by PSII fluorescence would not be re-absorbed. Then, PSI fluorescence excited by PSII fluorescence and detected at the surface would be half the PSI fluorescence:

$$dF_{\mathrm{I} \leftarrow F_{\mathrm{II}}} = I \cdot e^{-e_1 \cdot C} \cdot e_1 \cdot dC \cdot \frac{\phi_{\mathrm{II}}}{2} \cdot \frac{\phi_{\mathrm{I}}'}{2} \cdot [(1 - e^{-e_2 \cdot C}) + (1 - e^{-e_2 \cdot (C' - C)})] \qquad \text{Eq. A6}$$

where ϕ_{I}' denotes the PSI fluorescence yield excited by PSII fluorescence (See Fig. S2). PSI fluorescence directly excited by the actinic light and emitted by the thin layer at C (dC) can be detected by the sensor is expressed as:

$$dF_{\mathrm{I}\,direct} = \frac{\phi_{\mathrm{I}}}{2} \cdot I \cdot e^{-e_1 \cdot C} \cdot e_1 \cdot dC \qquad \text{Eq. A7}$$

where ϕ_{I} denote PSI fluorescence yield excited by blue light. Integration from 0 to

C' of these equations give:

$$F_{\mathrm{I}\,direct} = \frac{\phi_{\mathrm{I}}}{2}\int_0^{C'} I \cdot e^{-e_1 \cdot C} \cdot e_1 \cdot dC \qquad \text{Eq. A8}$$

$$F_{\mathrm{I}\leftarrow F_{\mathrm{II}}} = \frac{\phi_{\mathrm{II}}}{2} \cdot \frac{\phi_{\mathrm{I}}'}{2}\int_0^{C'} I \cdot e^{-e_1 \cdot C} \cdot e_1 \cdot \left[\left(1 - e^{-e_2 \cdot C}\right) + \left(1 - e^{-e_2 \cdot (C' - C)}\right)\right] dC \qquad \text{Eq. A9}$$

The ratio of these integrals is expressed as:

$$\frac{F_{\mathrm{I}\leftarrow F_{\mathrm{II}}}}{F_{\mathrm{I}\,direct}} = \frac{\phi_{\mathrm{II}}}{2} \cdot \frac{\phi_{\mathrm{I}}'}{\phi_{\mathrm{I}}} \cdot \frac{\int_0^{C'} I \cdot e^{-e_1 \cdot C} \cdot e_1 \cdot \left[\left(1 - e^{-e_2 \cdot C}\right) + \left(1 - e^{-e_2 \cdot (C' - C)}\right)\right] dC}{\int_0^{C'} I \cdot e^{-e_1 \cdot C} \cdot e_1 \cdot dC} \qquad \text{Eq. A10}$$

PSII fluorescence emitted in dC and reaches to the surface can be expressed, because we may neglect effects of PSII fluorescence emitted to the other side:

$$dF_{\mathrm{II}surface} = \frac{\phi_{\mathrm{II}}}{2} \cdot I \cdot e^{-e_1 \cdot C} \cdot e_1 \cdot dC \cdot e^{-e_2 \cdot C} \qquad \text{Eq. A11}$$

The absorption coefficients *in situ*, e_1 and e_2 may be estimated by examining the effects of the cumulated Chl concentration of the thylakoid suspension on PSI and PSII fluorescence. When we neglect the PSI fluorescence excited by PSII fluorescence, we obtain PSI fluorescence as Eq. A8.

$$\frac{\phi_{\mathrm{I}}}{2}\int_0^{C'} I \cdot e_1 \cdot e^{-e_1 \cdot C}\, dC = \frac{\phi_{\mathrm{I}}}{2} \cdot I \cdot \left(1 - e^{-e_1 \cdot C'}\right) \qquad \text{Eq. A12}$$

PSII fluorescence reaching the surface can be estimated by integrating Eq. A11:

$$\frac{\phi_{\mathrm{II}}}{2}\int_0^{C'} I \cdot e_1 \cdot e^{-(e_1 + e_2) \cdot C} \cdot dC = \frac{\phi_{\mathrm{II}}}{2} \cdot I \cdot \frac{e_1}{(e_1 + e_2)} \cdot \left(1 - e^{-(e_1 + e_2) \cdot C'}\right) \qquad \text{Eq. A13}$$

By curve fitting of the dependence of PSI and PSII fluorescence on C', e_1 and e_2 may be estimated (see Fig. S4 for the estimation of e_1).

The ratio (Eq. A10) is a function of PSII and PSI fluorescence yields and absorption coefficients. The ratio increases with C' (Fig. S5). Since PSII fluorescence little excites PSII fluorescence while preferentially excites PSI, ϕ_{I}' would be twice of ϕ_{I}. Then, Eq. A10 may become:

$$\frac{F_{\mathrm{I}\leftarrow F_{\mathrm{II}}}}{F_{\mathrm{I}\,direct}} \approx \phi_{\mathrm{II}} \cdot \frac{\int_0^{C'} I \cdot e^{-e_1 \cdot C} \cdot e_1 \cdot \left[\left(1 - e^{-e_2 \cdot C}\right) + \left(1 - e^{-e_2 \cdot (C' - C)}\right)\right] dC}{\int_0^{C'} I \cdot e^{-e_1 \cdot C} \cdot e_1 \cdot dC} \qquad \text{Eq. A14}$$

Then, ϕ_{II} is the key factor. The ratio of integrals is at most 1~2 (See Fig. S5). Because PSII fluorescence yield excited by blue light, ϕ_{II}, is small (Latimer et al. 1956, Lamb et al. 2018 and references therein), the effects of PSII fluorescence re-absorption on PSI fluorescence should be also small.

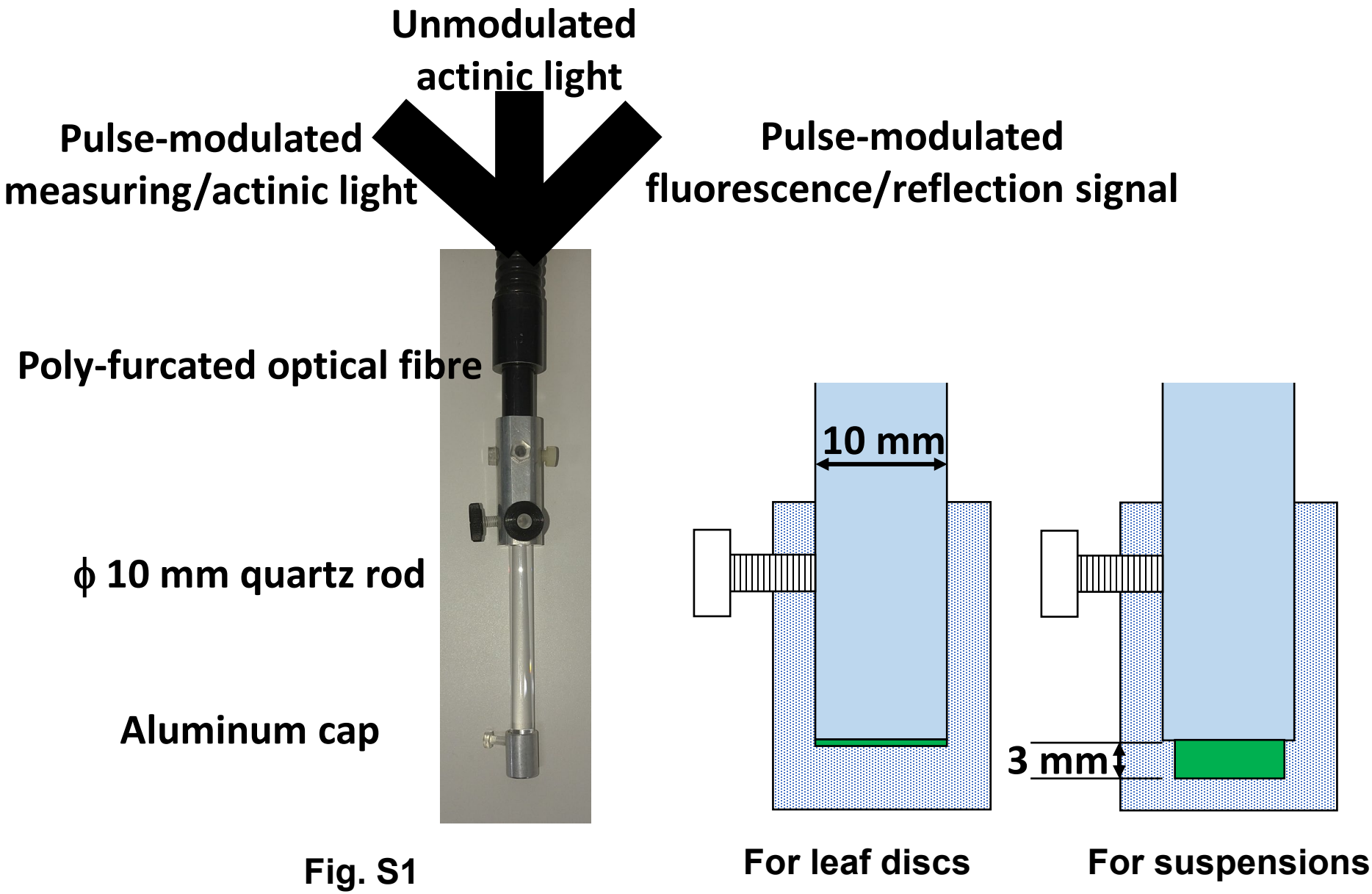

Fig. S1. The optics and cuvettes for fluorescence measurements.

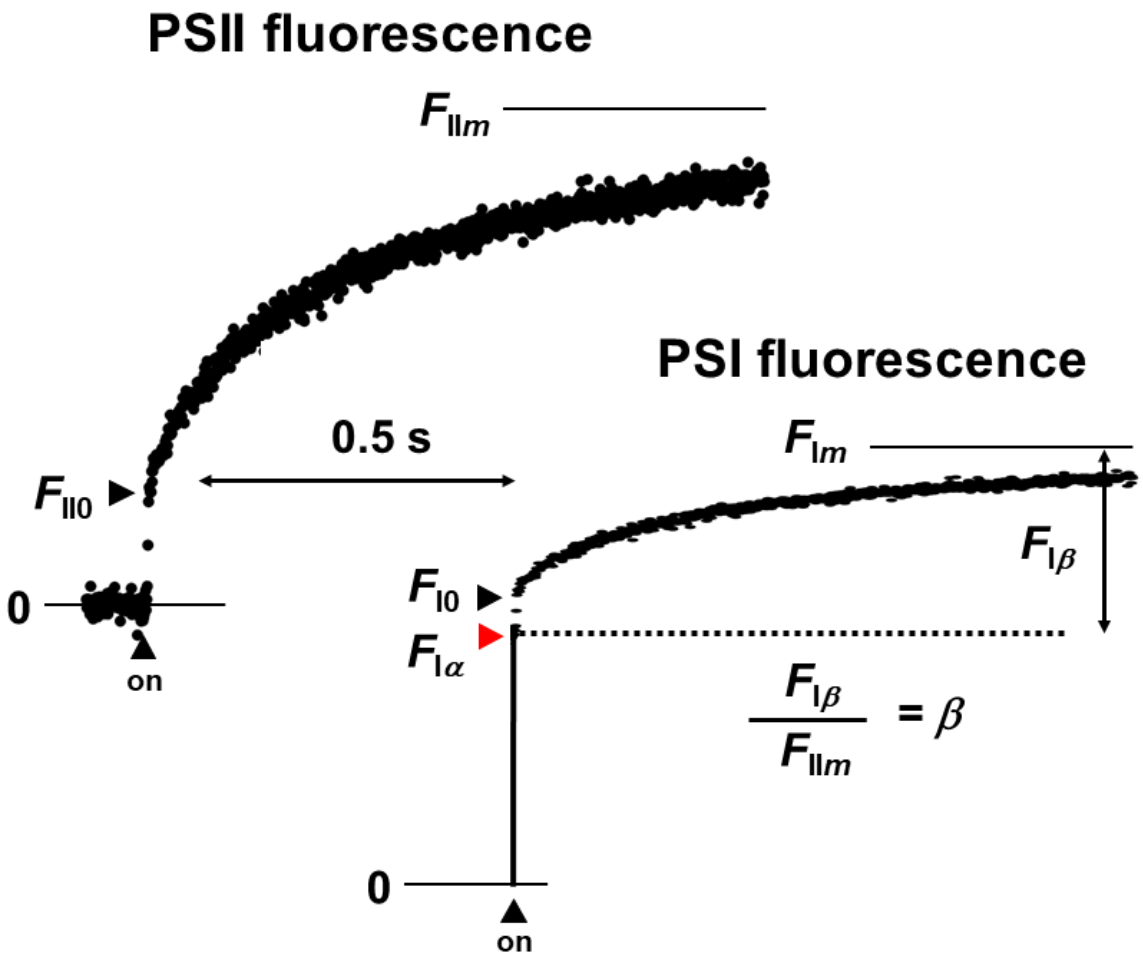

Fig. S2. Relationships between PSII and PSI fluorescence.
PSI fluorescence is assumed to be the sum of PSI intrinsic fluorescence, $F_{I\alpha}$, and that due to Chl*s spilt over from PSII, $\beta F_{II}(t)$: $F_I(t) = F_{I\alpha} + \beta F_{II}(t)$.
$F_{I\alpha}$ can be obtained as $F_{I\alpha} = F_{Im} - (F_{Im} - F_{I0}) \cdot \frac{F_{IIm}}{F_{IIm} - F_{II0}}$.

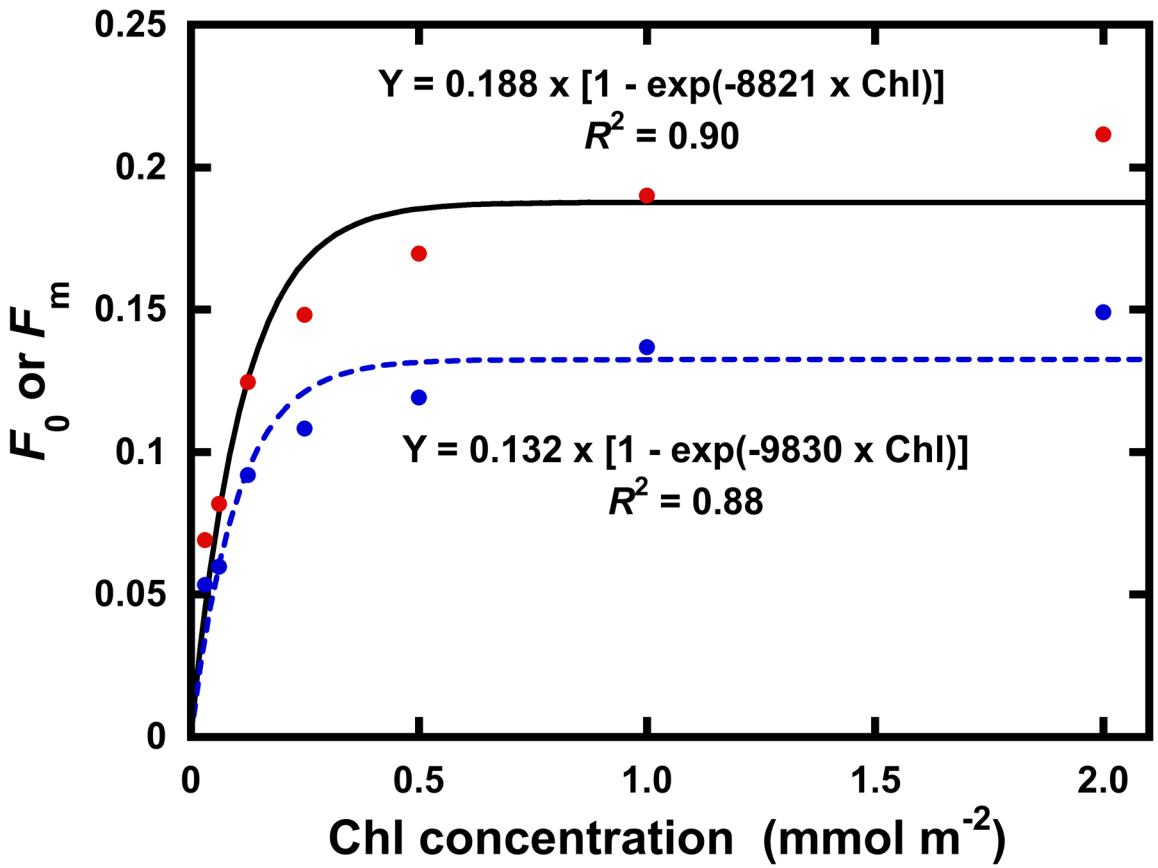

Fig. S3

Fig. S3. Determination of e_1. In this calculation, we assume no PSI fluorescence excited by PSII fluorescence.

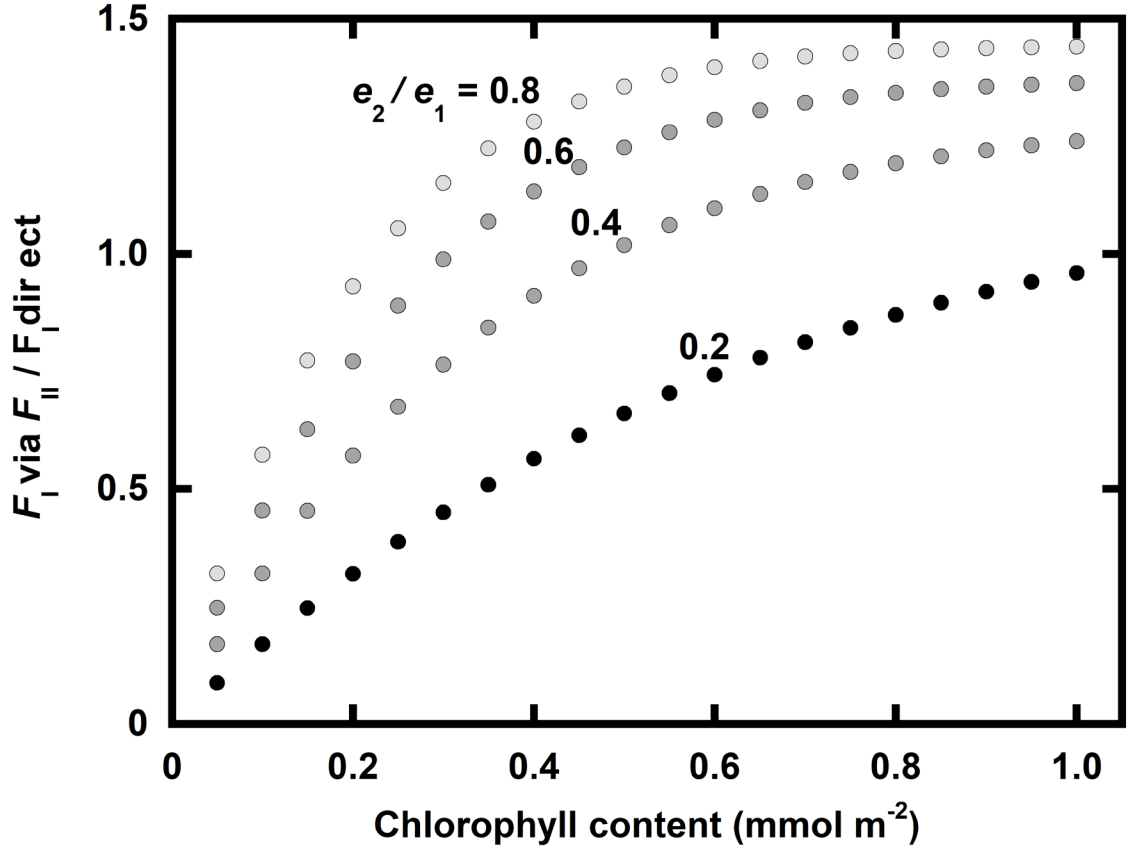

Fig. S4 The ratio of the integrations in Eq. S10 as a function of the Chl content.

$$\frac{\int_0^{C'} I \cdot e_1 \cdot e^{-e_1 \cdot C} \cdot [(1 - e^{-e_2 \cdot C}) + \left(1 - e^{-e_2 \cdot (C' - C}\right)] dC}{\int_0^{C'} I \cdot e_1 \cdot e^{-e_1 \cdot C} \cdot dC}$$

The ratio increases with the increase in C'. For e_1, we used 9000 (namely ε_1 of 9000/2.3 = 3913 m^2 mol^{-1}). We did not estimate e_2 experimentally. Several possible e_2 values were used (see Fig. S5).

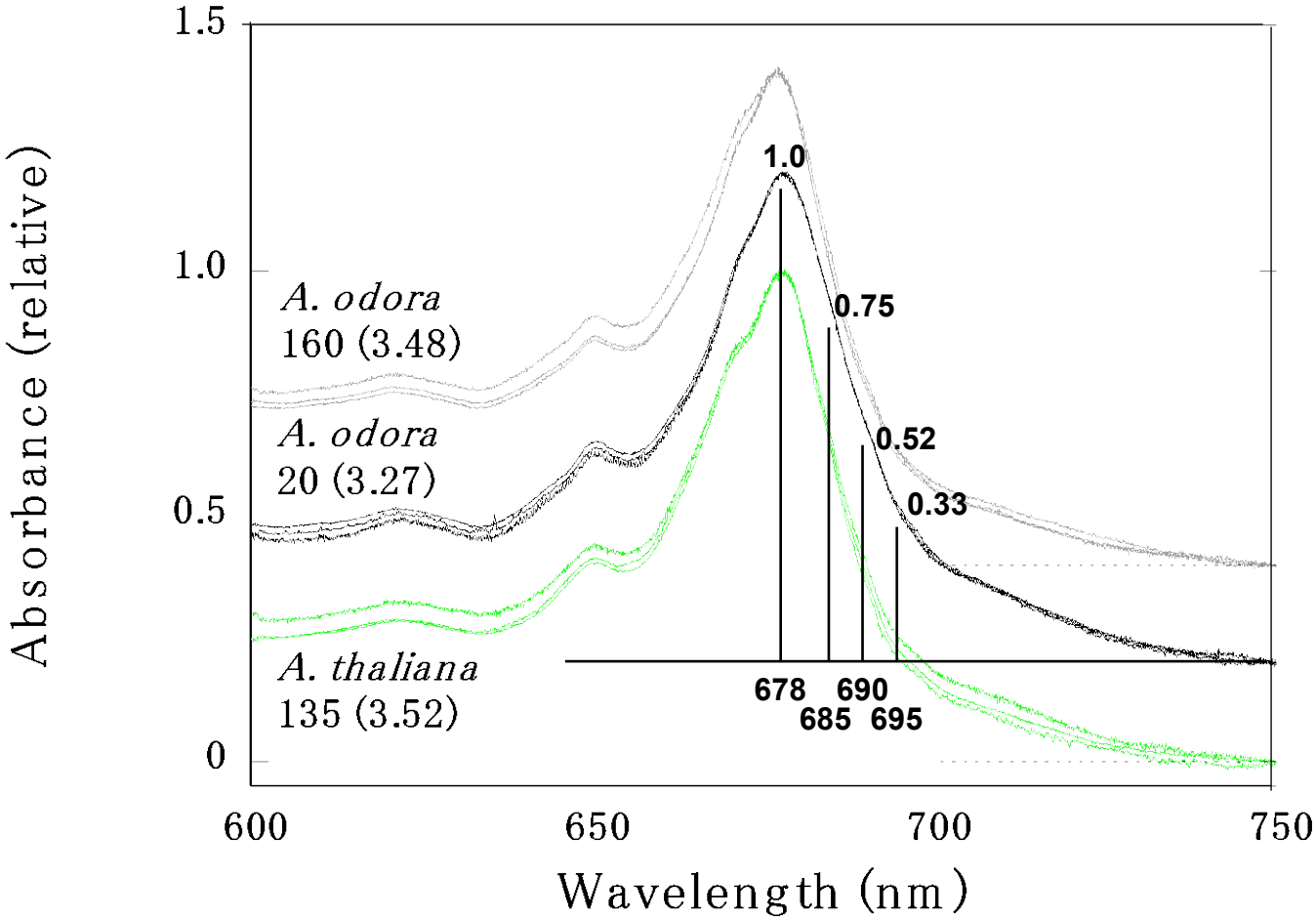

Fig. S5. 77K absorbance spectra of thylakoid suspensions prepared from the leaves of *A. odora* grown at 160 and 20, and *Arabidopsis thaliana* grown at 135 μmol m^{-2} s^{-1}. Assuming the red peak (678 nm) height is similar to that at 460 nm (REF), e_2 at 685, 690 and 695 nm were estimated for low-light *A. odora*. The original figure in Terashima et al. (2021) was modified by the authors.

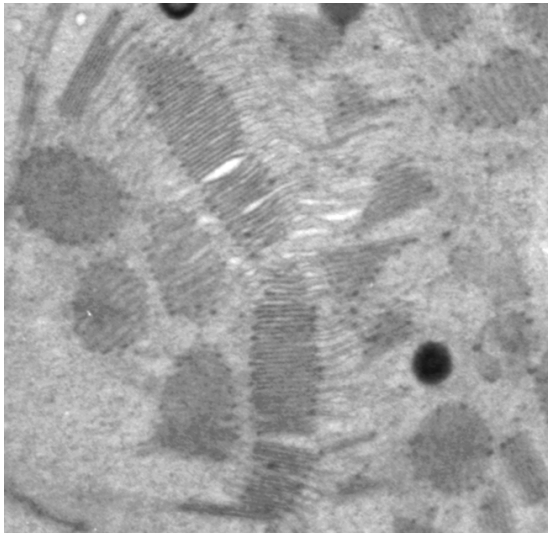

Fig. S6 A

A part of a HL-*A. odora* chloroplast. Determination of the length of non-appressed thylakoid membranes (NAP) and appressed thylakoid membranes (AP). The ratio of NAP to the total length (NAP+AP) was 0.424.

appressed

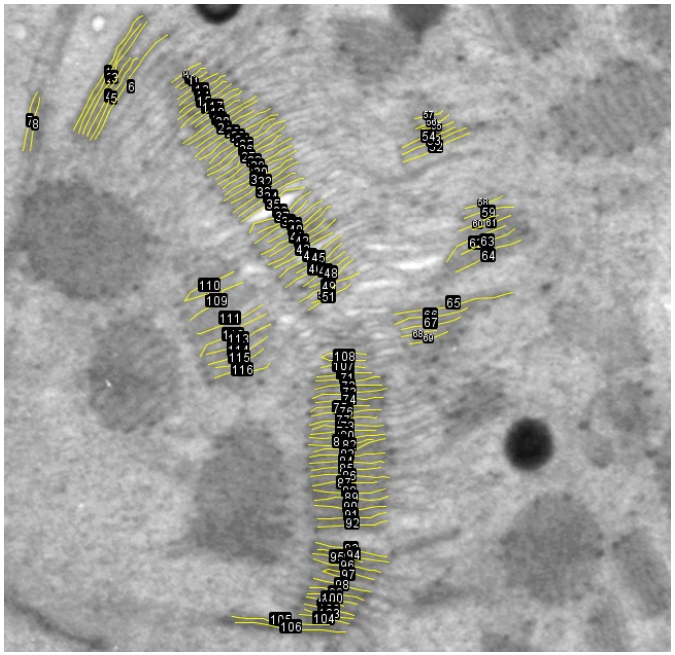

Non-appressed

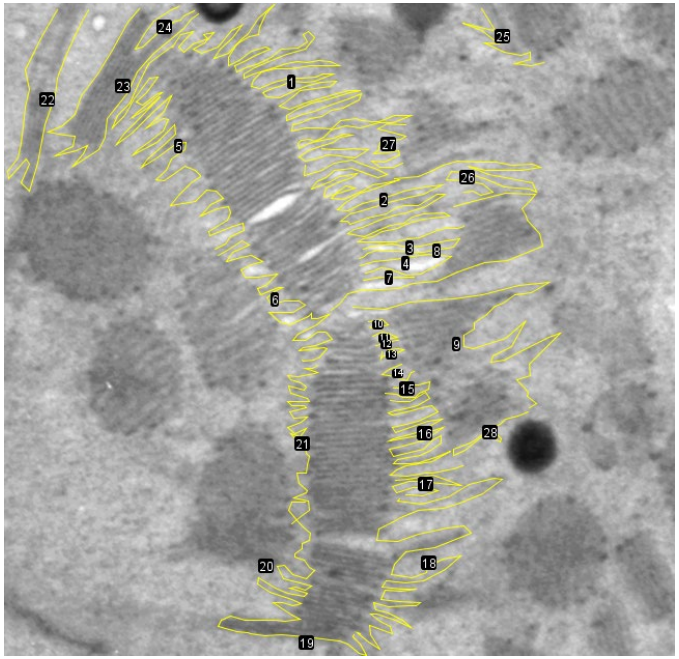

AP: 59.31
NAP: 43.738

NAP/T: 0.424

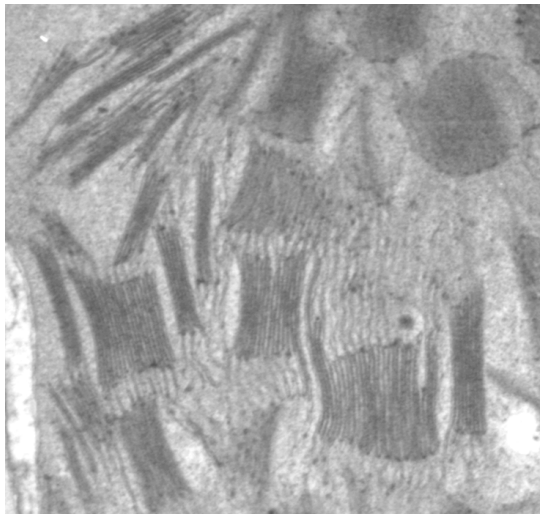

Fig. S6 B

A part of a LL-*A. odora* chloroplast. Determination of the length of non-appressed thylakoid membranes (NAP) and appressed thylakoid membranes (AP). The ratio of NAP to the total length (NAP+AP) was 0.41.

appressed

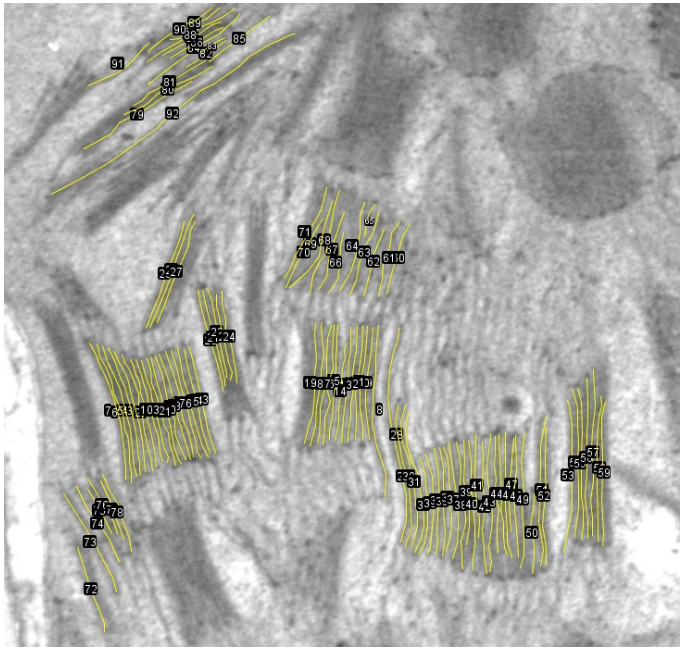

Non-appressed

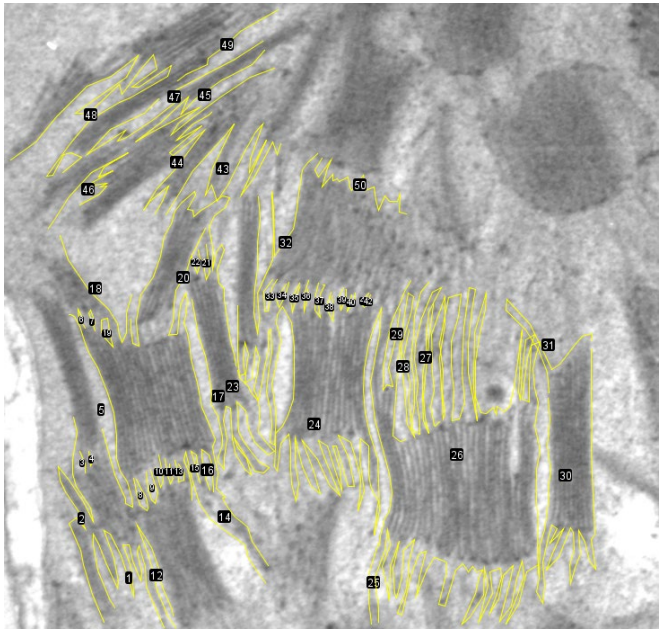

AP:
84.498
NAP:
59.337

NAP/T: 0.41